Open access • Journal Article • DOI:10.1116/1.1491722

Initiation of Electrical Breakdown in Ultrahigh Vacuum — Source link

D. Alpert, D. A. Lee, E. M. Lyman, H. E. Tomaschke

Published on: 01 Nov 1964 - Journal of Vacuum Science and Technology (American Vacuum Society)

Topics: Electrical breakdown, Electric current, Local field and Field electron emission

[redacted]

Coordinated Science Laboratory

UNIVERSITY OF ILLINOIS - URBANA, ILLINOIS

INITIATION OF ELECTRICAL BREAKDOWN IN ULTRAHIGH VACUUM

D. Alpert, D. A. Lee, E. M. Lyman and H. E. Tomaschke

REPORT R-234 AUGUST, 1964

COORDINATED SCIENCE LABORATORY
UNIVERSITY OF ILLINOIS
URBANA, ILLINOIS

The research reported in this document was made possible by support extended to the University of Illinois, Coordinated Science Laboratory, under the Joint Services Electronics Program by the Department of the Army, Department of the Navy (Office of Naval Research), and the Department of the Air Force (Office of Scientific Research), and by the Advanced Research Projects Agency under Department of the Army contract

DA-28-043-AMC-00073(E)

ABSTRACT

Existing theories for the initiation of electrical breakdown are reviewed, together with the experimental observations on which they are based. Experiments here described have extended the available data on electrical breakdown between broad area electrodes under ultrahigh vacuum conditions. The results, together with those of several other experimenters, are interpreted on the basis of a single picture which explains and relates the phenomena of predischarge currents and the initiation of breakdown. Based on field emission from sharp submicroscopic points, this picture predicts breakdown when the local electric field at the cathode reaches a critical value. The local field, which for broad area electrodes may be much larger than the average field, is deduced from observations of field emission prior to breakdown. When properly analyzed, data for tungsten electrodes from this research and several others indicate a value for the electrical field at breakdown which is independent of gap spacing or geometrical configuration for voltages up to 250 kV. The critical breakdown field for tungsten is 6.5×10^7 V/cm. The above picture also gives physical insight into other phenomena associated with electrical breakdown.

TABLE OF CONTENTS

EB-1964

I. INTRODUCTION

Although vacuum can act as a good insulator between metal electrodes at low voltages, it has been found that as the voltage is increased, there is a relatively reproducible value at which a transition to a high current, low voltage arc takes place. At sufficiently low pressures it has been found that the initiation of the arc, referred to as electrical breakdown, is independent of the residual gas and appears to be determined by the properties of the electrode surfaces.

The literature on electrical breakdown contains quantitative data on electrode-dominated voltage breakdown as early as the turn of the century.[1] In 1918, Millikan and Sawyer[2] reported some of the earliest quantitative measurements on breakdown at low pressures. They summarized this work (undertaken as early as 1905) as follows: "The potential difference required to produce these hot sparks, amounting to 150,000 V/mm under certain circumstances, were independent of the residual gas pressure, provided this was sufficiently low, for example, between 10^{-5} and 10^{-8} mm of Hg." Millikan went on to describe certain observations which later experimenters have called "electrode conditioning."[3]

Since the very early work mentioned above, a large number of researchers have made measurements relating to the dependence of electrical breakdown on various parameters. A summary of some of the experimental contributions is indicated in Figure 1, which gives data from a very wide number of sources[4-14] for breakdown voltages as a function of two very important parameters, (1) gap spacing, and (2) electrode material. The

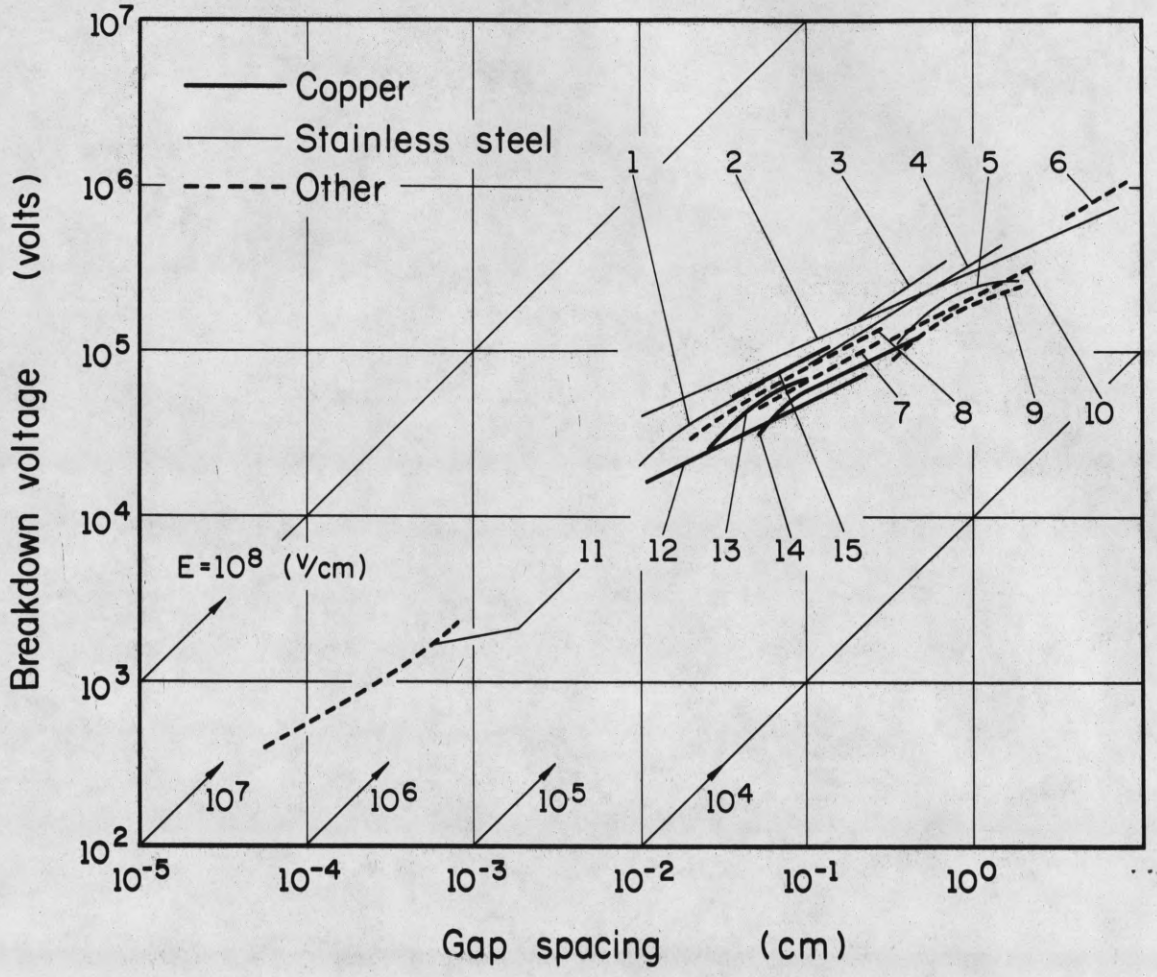

Fig. 1. Breakdown voltage versus gap spacing for various electrode materials. The results of various experimenters are here indicated on a single plot for comparison.

1. Denholm, steel, see footnote 4.
2. Trump, stainless steel, see footnote 5.
3. Slivkov, steel, see footnote 6.
4. Anderson, stainless steel, see footnote 7.
5. McKibbon, stainless steel, see footnote 8.
6. Heard, inconel, see footnote 13.
7. Rosanova, iron, see footnote 12.
8. Rosanova, molybdenum (5 to 3 x 10^{-5} cm), see footnote 12, and Denholm, aluminum (2 to 8 x 10^{-5} cm), see footnote 4.
9. McKibbon, steel, see footnote 8.
10. McKibbon, aluminum, see footnote 8.
11. Boyle, Kisliuk, Germer, tungsten, see footnote 14.
12. Myers, copper, see footnote 11.
13. Denholm, copper, see footnote 4.
14. Pivovar, copper cathode, lead anode, see footnote 9.
15. Parkins, copper, see footnote 10.

many subsequent experimenters have added to the overall information available, notably that the breakdown field appears to depend on gap spacing, evidence for which was first provided by Anderson.[15] It will be noted, however, that in the 40 years of research since Millikan's early observations, there has been virtually no improvement in the value of breakdown field strengths available for the range of gap spacings of greatest interest.

Among the problems which have made progress difficult have been the experimenters' lack of ability to control or measure such factors as the microscopic and atomic nature of the electrode surfaces, the residual gas pressure, and the surface contamination during the course of an experiment. Thus, despite the large volume of data made available, there have been relatively few definitive experiments which uniquely identify, or alternatively, which uniquely exclude a specified a specified physical process which may lead to the initiation of breakdown. Even with such an obvious parameter as the electrode material, it has not been possible to ascribe the differences in the observed breakdown characteristics solely to the properties of the electrode material. For example, it can be seen from Figure 1 that the measurements taken with the same electrode material by different experimenters may have a larger variation than the corresponding results of a given experimenter taken for several different electrode materials. In view of the nature of such results, there was a tendency in the early literature to interpret a given experiment in terms of one or another phenomenological picture for breakdown, each model requiring a suitable choice of adjustable parameters to fit the gross features of the experimental observations. Due to the continued interest of many competent

workers over the years, there is no shortage of postulated mechanisms for the observed phenomena. However, in view of the many unspecified conditions noted above, it is not surprising that the literature on electrical breakdown has produced few theoretical explanations supported by convincing experimental proof.

The development of the field emission microscope[16] and the introduction of ultrahigh vacuum techniques,[17] made it possible in the early fifties to carry out certain experiments in which contamination from the vacuum system and the effects of residual gases could be eliminated or controlled, and the nature of the cathode surface specified in detail. With these techniques at their disposal, Dyke and his co-workers, Barbour, Dolan, Martin, and Trolan,[18,19,20] were able to carry out the first (and only) set of experiments in which the initiation of breakdown can be unambiguously associated with a specified physical process. These experiments were carried out with a point-to-plane geometry similar to that in a Müller field emission microscope; the electrode material and its structure could be accurately defined, the geometry could be specified to the dimensions identifiable in an electron microscope, and the cathode surface could be atomically cleaned and maintained in this condition throughout the course of the experiment.

Dyke and his colleagues obtained values for the electric field at breakdown of approximately 7×10^7 V/cm, a value one or two orders of magnitude higher than that found for more typical electrode geometries and vacuum conditions. Furthermore, they were able to demonstrate in a conclusive way that breakdown in the point-to-plane geometry is initiated by

the resistive heating of the cathode tip by field emission currents. It is interesting to note that this is a process which had been postulated almost two decades earlier.[21]

The papers of Dyke and his co-workers, written almost a decade ago, were immediately recognized for their definitive quality. However, the results which they described were so different in a quantitative sense from those in the existing literature that the phenomena in the different geometries did not seem to be related. In any case, neither Dyke nor other workers in the field have hitherto made a serious attempt to relate this work to other geometries or to previous work in electrical breakdown.

The research program to be described in this paper was aimed at an understanding of the physical processes which are responsible for the initiation of electrical breakdown between broad area electrodes, i.e., for electrodes whose dimensions are comparable to the gap spacing between them. It was particularly intended to examine experimentally whether modern vacuum techniques and recent advances in the study of clean surfaces could bring new insight into the problem. With the encouragingly high values for breakdown field demonstrated by Dyke and his co-workers, it was especially of interest to relate this work involving point-to-plane geometries to that for other geometries. With the above factors in mind, the material selected for most detailed investigation was tungsten, and most of the results and conclusions were obtained from studies with electrodes of this material.

The results of the present investigation are discussed in two main parts. Part I, the present paper, is devoted to a description of the role

of field emission in electrical breakdown, an essential feature of which is the existence or formation of multiple points or whiskers on the broad area electrodes. It should be quite evident from the introduction above that there is no intent here to claim priority for the proposal that such projections on metallic electrodes play an important role in electrical breakdown, or that they may greatly enhance the field emission. Rather, it is herein intended to present a physical picture which quantitatively relates predischarge characteristics to the initiation process, together with supporting experimental evidence for this interpretation of the initiation process. An accompanying paper, hereafter referred to as II, will describe a series of studies which were suggested by, and are complementary to those in I. They involve detailed experimental and analytical investigations of the projections on electrodes and their effects on electrical breakdown in vacuum.

II. SOME THEORIES FOR THE INITIATION OF BREAKDOWN

A. Field emission

As indicated in section I, an unambiguous explanation of the observed predischarge currents and of the breakdown voltage is available for a point-to-plane geometry under ultrahigh vacuum surface conditions. To explain the predischarge currents, Dyke and his co-workers[18,19,20] showed that as the electric field at a clean single-crystal tungsten-point cathode is varied, the current drawn to the anode accurately follows the predictions of the Fowler-Nordheim theory[22,23] for field emission. This theory, which describes the process as a quantum mechanical tunneling of conduction electrons through the potential barrier at the surface of the metal, gives the following expression for the dependence of current density, J, on electric field:[24]

$$J = -\frac{1.54 \times 10^{-6} E^2}{\varphi t^2 \left(\frac{3.79 \times 10^{-4} E^{1/2}}{\varphi}\right)} \exp -6.83 \times 10^7 \frac{\varphi^{3/2}}{E} v \left(3.79 \times 10^{-4} \frac{E^{1/2}}{\varphi}\right) \qquad (1)$$

where:

E is the electric field at the cathode surface,

φ is the work function of the cathode material, and

v and t are slowly varying functions which are almost constant over the useful range of measurements of the current density.

In Dyke's experiments, the point cathode was carefully prepared by electrolytically etching the tip of a small tungsten wire to a fine point. This was then heated to a high temperature in ultrahigh vacuum to anneal out the imperfections, thus producing a single crystal. The shape of the smoothed point, whose radius was typically less than 10^{-4} cm, was determined with an electron microscope.[25] This information made possible an accurate calculation of the electric field at the emitter surface. The shape of the cathode was preserved even at high current densities by pulsing the voltage at the higher values, thus limiting the heating effects and minimizing surface migration. The anode was located at a distance of several centimeters from the cathode.

By measuring the current as a function of applied voltage, Dyke and his colleagues verified the Fowler-Nordheim theory over a range of at least six orders of magnitude in current, from 6 A/cm^2 to 6 x $10^6 A/cm^2$, and showed that the small deviation from the equation for greater values of current could be explained on the basis of space charge alteration of the field at the surface. The curve was reproducible and reversible for current densities up to 10^8 A/cm^2. At this critical value of current density (10^8 A/cm^2), a sharp discontinuity in current was observed, rising by at least two orders of magnitude in a time less than 50 nanoseconds. Thereafter, the emission characteristics of the cathode were greatly altered, and examination under the electron microscope indicated that the point had been violently destroyed. Dolan, Dyke, and Trolan[20] explained the electrical breakdown in these experiments as due to the resistive heating of the cathode to the melting point of the tungsten. They made calculations

to show that the field currents of this magnitude can indeed heat the tip to the melting point in less than the microsecond pulse duration used in these experiments.

On the basis of the chosen values of gap spacing and the observed rate of current build-up, they were able to demonstrate that the anode played no role in the initiation of the high current "arc," the gap spacing being too large to permit the transfer of neutral or of charged particles heavier than hydrogen ions in a time less than 5×10^{-8} sec. Hence, the above results provided incontrovertible evidence that field emission was responsible for the initiation of breakdown.

If questions remain as to the interpretation of the Dyke experimenta, they lie in the authors' explanation of the formation of the arc, i.e., the rapid change in current which accounts for the destruction of the point cathode. This rapid current rise is attributed to the sudden onset of space charge neutralization provided by ions formed in the metallic vapor evaporated at the point cathode. However, Dyke et al. do not explain why there should be a discontinuity in the production of ions or in the vapor pressure of the tungsten at its melting point. In the first place it should be noted that the vapor pressure of a metal does not suffer a a discontinuity at the melting point; in the second place, the vapor pressures at the melting point of common electrode materials differ by over ten orders of magnitude. Hence, significantly different behavior from that for tungsten would be expected for other materials, a result which is not typical of breakdown data. Finally, the Dyke group did not describe in detail the mechanism by which ions, even if produced in quantity, could

account for the magnitude of the current rise. It would seem, therefore, that an explanation of the detailed processes leading from initiation to the final arc (or the destruction of the cathode) may lie in other directions, for example, the sudden change in the mechanical properties of the cathode at the melting point of the cathode tip. Alternative explanations are considered in II.

Before introducing a picture for the initiation process for broad area electrodes based on field emission, it is instructive to review briefly certain other theories which have continued to receive serious attention. The reasons for considering other mechanisms is based on certain observations which on first glance the field emission hypothesis did not seem to explain. Among such observations are the following:

1. Dependence of breakdown voltage on gap spacing. As shown in Figure 1, the observed values of breakdown voltage does not vary linearly with gap spacing. Thus the average value of the electric field at breakdown does not appear to be constant, but to vary with the position of the anode.
2. Anode material. In addition to the dependence on the position of the anode, the breakdown voltage between broad area electrodes seems to be affected by the nature and condition of the anode surface.
3. Material transfer between electrodes. Many researchers[26] have observed that material may be transferred from anode to cathode or vice versa upon the application of high voltage, even at values below that at which breakdown occurs.

4. The magnitude and nature of predischarge currents. In general, the currents drawn between electrodes are many orders of magnitude higher than those expected from a simple application of the Fowler-Nordheim theory. Although the current is typically carried by particles of negative charge, there are some experiments which have indicated charge carriers of both signs.

In view of such observations, three other hypotheses for the initiation process have received wide-spread attention, one based on regenerative processes at the electrode surfaces, the second based on the transfer of massive particles between electrodes, and the third based on localized heating of the anode.

B. Surface regeneration processes

Van Atta and Van de Graaff[27] have proposed as an initiating event for breakdown the interchange of charged atomic particles between cathode and anode, that is, a chain reaction in which particles ejected from one electrode produce particles of the opposite sign upon impact at the other electrode surface. Breakdown occurs when the regeneration coefficient, i.e., the product of the cross-sections for the generation of particles at the respective surfaces, exceeds unity.

Although this process has been under serious investigation for several decades, positive evidence for a surface regeneration effect has been provided only in a limited number of investigations. Arnal[28] and Mansfield and Fortescue[29] have shown that under certain conditions,

particularly under poor vacuum conditions, current may flow between the electrodes at voltages well below the threshold for breakdown. Since the current flows as self-extinguishing pulses (of millisecond duration), some authors have used Arnal's term "microdischarges" to describe the effect. Both Arnal and Mansfield and Fortescue found evidence for an exchange process involving the production of positive ions at the anode and negative ions at the cathode.

Recent observations[30] (incident to the development of high energy particle separators) also seem to indicate a particle interchange process which produces a quasi-stable glow discharge taking the form of a diffuse column extending from one electrode to the other, or of a somewhat mobile luminous patch close to the surface of the electrodes. Rohrback and Germain noted that the columns, about 1 to 2 cm in diameter, move about over the surface during the early stages of vacuum conditioning, and eventually disappear. If unusually persistent, the effect could be removed by carefully cleaning the electrodes. Murray found that the luminous patches were unaffected by the imposition of a weak magnetic field transverse to the electric field, thus providing evidence in support of ion exchange between the plates. Similar observations have been made by one of us (EML) on the ZGS particle separators at the Argonne National Laboratory. In addition, it was found upon removing them, that pairs of "conditioned" plates, i.e., electrodes which no longer sustain such a localized glow, have complementary discoloration patterns; a discoloration region on one electrode is qlways faced by a completely clean region of the same size and shape on the opposite plate. This suggests that ion exchange

can occur only if both plates have contaminated surfaces, and ceases as soon as either electrode is cleaned by the action of bombarding particles.

In general, such conduction does not lead to a destructive discharge, but to a drain on the power supply at voltages well below "breakdown." A number of experimenters[32,33,34,35] have demonstrated that for conditioned surfaces, the measured cross-sections are far too small to support a regenerative mechanism. Pivovar and Gordienko[31] showed rather conclusively that conduction of this type is absent when surface contamination is minimized through the use of modern ultrahigh vacuum techniques. At relatively low voltages (up to 12 kV) Raether,[36] of our laboratory, has shown that under ultrahigh vacuum and clean surface conditions, the ratio of positive to negative current does not exceed a value of 10^{-6} up to the point of breakdown. From the above discussion, it will be noted that, although considerable evidence exists that a regenerative process may cause a large predischarge current between highly contaminated surfaces, experimental observations seem to exclude surface regeneration as a cause of electrical breakdown. Not only are the measured values of the appropriate cross-sections too small to account for breakdown, but the measured dependence of cross-sections on particle energy fails to explain the observed variation of breakdown voltage as a function of gap spacing.

C. The Clump Hypothesis

Upon plotting the results of a large number of experimenters in a manner such as is shown in Fig. 1, Cranberg[37] noted that the data seemed to follow a square root law variation of breakdown voltage (V_b)

with gap spacing (d), i.e.,

$$V_b = Cd^{1/2} , \qquad (2)$$

where C is a constant of proportionality. This is, of course, a major departure from the linear dependence of V_b on d which would be characteristic of a mechanism solely associated with the electric field.

To explain this dependence, Cranberg postulated the so-called "clump hypothesis," attributing the initiation of breakdown to the transfer of charged clumps of material ripped from one of the electride surfaces and accelerated to the opposite electrode. If the particle is given sufficient energy, he concluded that it may produce upon impace localized "temperatures in excess of any known boiling points." Cranberg then showed that the energy transferred by a clump of material is proportional to the produce of the voltage through which the particle falls and the electric field at the surface from which it originated. The criterion for breakdown then becomes

$$V\ E \geqslant C^2 \qquad (3)$$

which is equivalent to (2) above, if one assumes E = V/d. Since Cranberg's presentation, other investigators have derived alternate expressions for the dependence of V_b on gap spacing, developing a somewhat different criteria for the required clump energy based on other assumptions as to the details of the initiating process. Slivkov[38] arrives at a somewhat different formulation for the breakdown criterion: $V_b = C\ d^{5/8}$,

where C is derived in terms of other physical constants. His derivation is based on the premise that if breakdown is to occur, it must take place in the vapor of the metallic particle and hence must meet the Townsend criterion for minimum sparking potential.

Alpert and Lee[39] calculate the constant of proportionality for Cranberg's criterion by assuming that breakdown will occur when the kinetic energy of the particle is sufficient to vaporize the particle through the work of compression. They give a formulation for the constant C in terms of physical parameters such as the modulus of compressibility, the density and the heat of sublimation.

There is every reason to believe that if the voltage applied between the electrodes is raised to a sufficiently high value, the forces exerted at the surface will eventually exceed the tensile strength of the electrode material itself, thus destroying the electrode in a single catastrophic event. Müller has, in fact, shown that such[24] a failure may take place even for a single crystal tungsten anode, at a field of about 5×10^8 V/cm.

However, in the range of voltages and gap spacing of typical interest, there is little direct evidence for the Cranberg mechanism. The most convincing indirect evidence is, as has been previously noted,[26] the observed transfer of metal from one electrode to the other. On the other hand, in attempts to verify the clump hypothesis by measuring the transit times for such macroscopic particles, Raether[36] obtained a totally negative result. Out of several thousand breakdowns induced by pulsed overvoltages, he found no correlation which could ascribe the initiation

to the transit of such a particle across the gap. This experiment was carried out with clean tungsten electrodes with total voltages up to 60 kV. Perhaps the only direct evidence for clump transfer as an initiator of discharges was provided by Heard and Lauer,[40] who were able to induce breakdown by injecting free particles into the electrode region with the high voltage on. In other words, the transfer of a charged particle between electrodes may be a sufficient condition, but not a typical or necessary precursor of breakdown.

One of the questionable conclusions from the Cranberg presentation is the predicted dependence of breakdown voltage on gap spacing. This arises from the assumption that the electric field at the surface of a loosely bound projection is the average field given by V/d. As will be seen from the discussion in the following sections, it is much more likely that the field at such a loosely bound particle will be strongly enhanced, and that the enhancement factor will itself depend on the gap spacing. Thus a more valid analysis of the process would lead to a quite different prediction for the dependence of breakdown voltage V_b on the gap spacing d.

D. Electron beam effects

A fourth approach to the explanation of electrical breakdown has involved the interaction at the anode of a beam of electrons originating at the cathode. The original paper describing the pinch effect in plasmas was written by Bennett[41] to explain electrical breakdown. In this paper, Bennett described the process of breakdown as due to a beam of electrons originating from field emission from point projections on the cathode.

The electron beam is then said to be confined to a very narrow column as a consequence of magnetic self-focusing which also confines the returning ions to a localized region. The impinging ions are then responsible for the initiation of the arc. It is not to detract from the importance of this paper in other implications to indicate that it is highly doubtful that a pinch can take place in an electron beam emitted from a point projection in view of the relatively high transverse velocities.

Boyle, Kisliuk and Germer,[42] in a paper which gives important insight into the nature of field emission from broad area electrodes, ascribe breakdown to the localized heating of the anode by impinging electrons. Their experiments involve very small gap spacings, for which beam spreading due to space charge is not large. Maitland[43] gives a similar explanation. However, this interpretation seems subject to serious question in view of calculations of Vibrans,[44] who has made an analysis of the spreading of an electron beam due to space charge. His analysis leads to the conclusion that for a specified gap spacing the maximum possible power density at the anode occurs when the cathode current density is about 10^4 A/cm^2. Since the results of Boyle, Kisliuk, and Germer as well as our own indicate that the cathode current density at breakdown is of the order of 10^7 A/cm^2, considerable doubt exists as to the possibility that localized anode heating plays a major role in initiating high voltage breakdown, particularly at large gap spacings.

In summary, although each of the alternative explanations of breakdown for broad area electrodes seems to have attractive features, we have adduced evidence, either experimental or theoretical, which subjects them to serious question.

III. A FIELD EMISSION PICTURE FOR BROAD AREA ELECTRODES

The work of Dyke and his collaborators showed that for point-to-plane geometry in clean systems, the measured values of predischarge currents and of breakdown voltage could be quantitatively explained by a straightforward picture based on field emission. As can be seen from the data for broad area electrodes in Figure 1, two significant departures from Dyke's results seem immediately evident. First, the electric field at breakdown (as defined by the expression $E_b = V_b/d$) is at least an order of magnitude lower than that of Dyke et al., and second, the breakdown field, E_b, varies with d, the breakdown field decreasing with increasing gap spacing. As to the predischarge currents, it has been typically observed that for broad area electrodes, the measured current exceeds that predicted by the Fowler-Nordheim theory by many orders of magnitude.

Since many of the researches in this field were carried out under conditions which differed markedly from those of Dyke et al., both as to the electrode material and the vacuum conditions, we singled out for special study[45] the investigation described by Boyle, Kisliuk and Germer,[42] in the paper hereafter referred to as BKG. The experiments of BKG were uniquely suitable for a comparison with those of Dyke et al., since they also utilized tungsten electrodes which could be maintained atomically clean through the use of ultrahigh vacuum techniques. They also used pulsed techniques to prevent undue heating of their electrodes, which were in the shape of crossed tungsten wires of small diameter (0.75 mm). Nevertheless, these are considered "broad area" in the sense that the gap spacings used were smaller than or comparable to the dimensions of the electrodes.

Let us first consider the BKG data on predischarge current. Figure 2 shows their results for current as a function of voltage for a gap spacing of 2×10^{-4} cm, plotted in a manner suggested by the field emission equation. It is seen, first of all, that the data follows a dependence rather closely analogous to that predicted by the Fowler-Nordheim expression. As was the case for Dyke's results, there is some departure, attributed to space charge saturation, from a straight line at higher values of current. However, the absolute values of the current are more than 15 orders of magnitude higher than would be expected from electrodes of these dimensions at an average field given by the voltage divided by the gap spacing. Furthermore, BKG demonstrated that the currents varied in an anomalous way as a function of gap spacing; i.e., the average field (V/d) required to draw a given current varied strongly with the gap spacing, d. BKG explained these anomalous effects, and brought their results into agreement with the Fowler-Nordheim theory by postulating that the current was drawn from an emission site which was very minute in area, (3×10^{-11} cm^2 for the data shown in Fig. 2) and that the electric field at the emission site exceeded the average electric field by an enhancement factor, ß, which ranged from unity at gap spacings of a few angstroms up to values as high as 30, as shown in Fig. 3. They explained the observed variation of field enhancement with gap spacing as due to enhancement of the electric field at small projections on the surface of the cathode. The alternate possibility of small areas of extremely low work function was rejected, since this would not be expected to be gap dependent.

Although this elegant analysis of the predischarge currents clearly associated conduction with field emission from sharp projections,

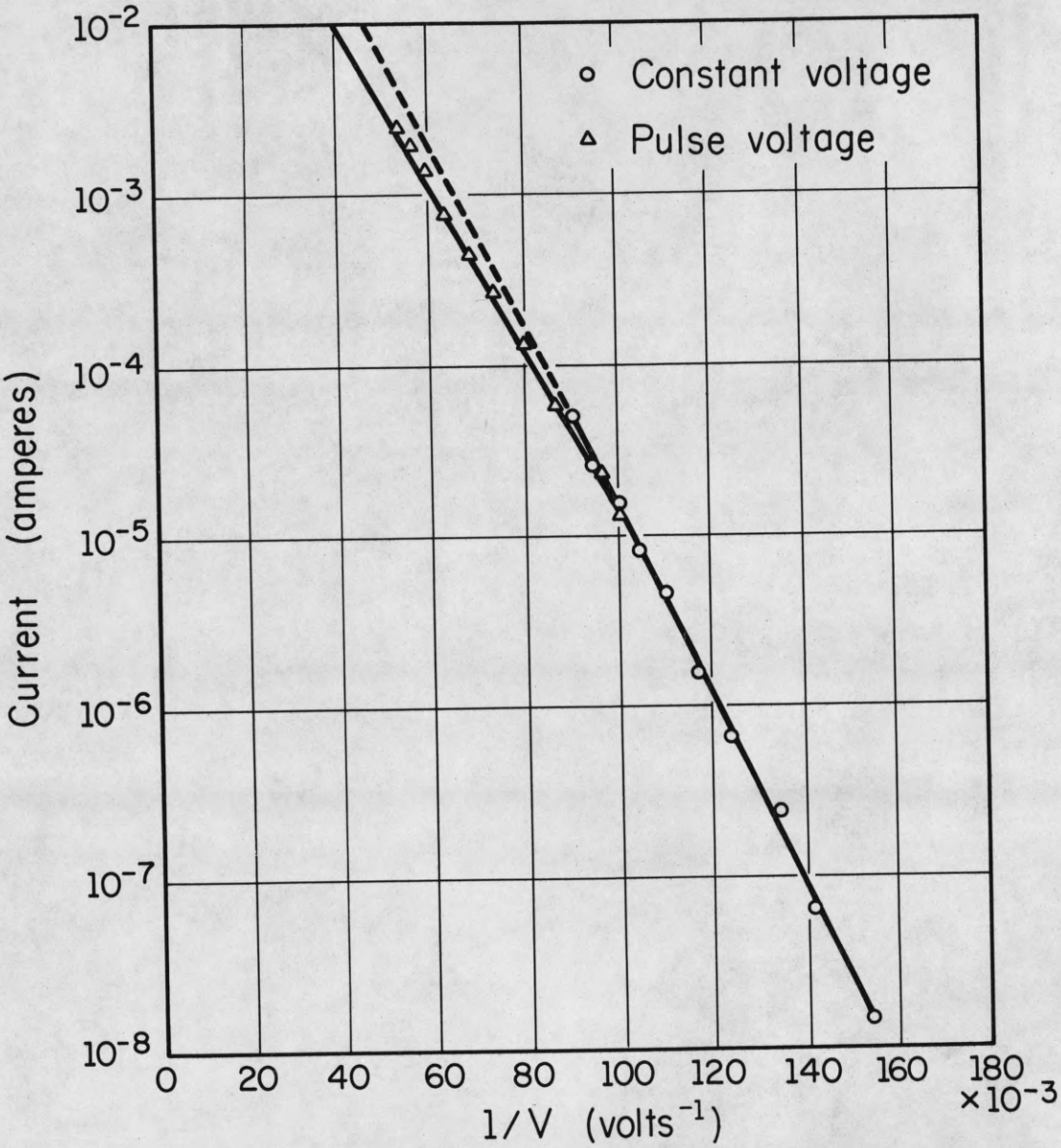

Fig. 2. Field emission current plotted as a function of reciprocal voltage as given by BKG.[14] Note that this is not a true F-N plot since the coordinate values are values of current rather than current divided by the square of either the voltage or the field. However, departure from F-N equation is not significant.

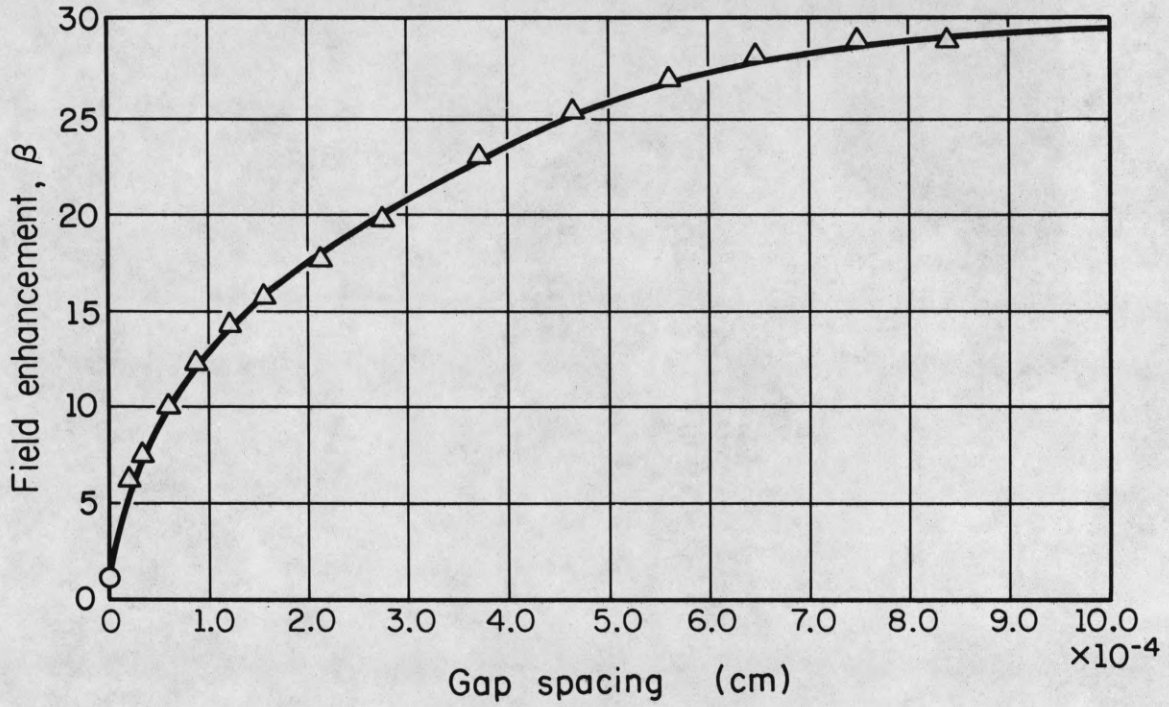

Fig. 3. Field enhancement factor, ß, as a function of gap spacing for extremely small spacing as given by BKG.[14] Zero gap spacing is given by the point of electrical contact.

BKG did not ascribe breakdown to the same mechanism as that proposed by Dyke. Their reasons for this were based on certain of their observations of current variation near breakdown, the interpretation of which may be open to question. Since we found the evidence for the process proposed by BKG, namely, localized heating of the anode, rather inconclusive, we were motivated to further comparisons of the BKG data with those of Dyke.

Such a comparison is shown in Figure 4 (curve A), in which the measured average breakdown field, V_b/d, is plotted as a function of gap spacing, d. As might be expected, the average field at breakdown varies strongly with gap spacing. However, if one multiplies the values of field by the corresponding value of the enhancement factor as taken from BKG's data in Figure 3, one obtains a measure of the true local field at breakdown. This has been done for each of the points on the curve 4A, as is shown in the upper curve, 4B. One obtains the interesting result that the "true" local breakdown field as derived from the observations of BKG has a constant value independent of gap spacing, and is equal to the value measured by Dyke within the experimental error.

This agreement in the value and gap invariance of breakdown field as obtained from the data of BKG and of Dyke et al., which had heretofore not been noted, suggested the picture for breakdown on which the present program was based. This picture follows BKG in the description of predischarge currents as due to field emission from projections on the cathode surface, although a significant departure from the simplified BKG picture of a single whisker was called for. (In the course of the research, it became evident that for broad area cathodes, the total emission arises from

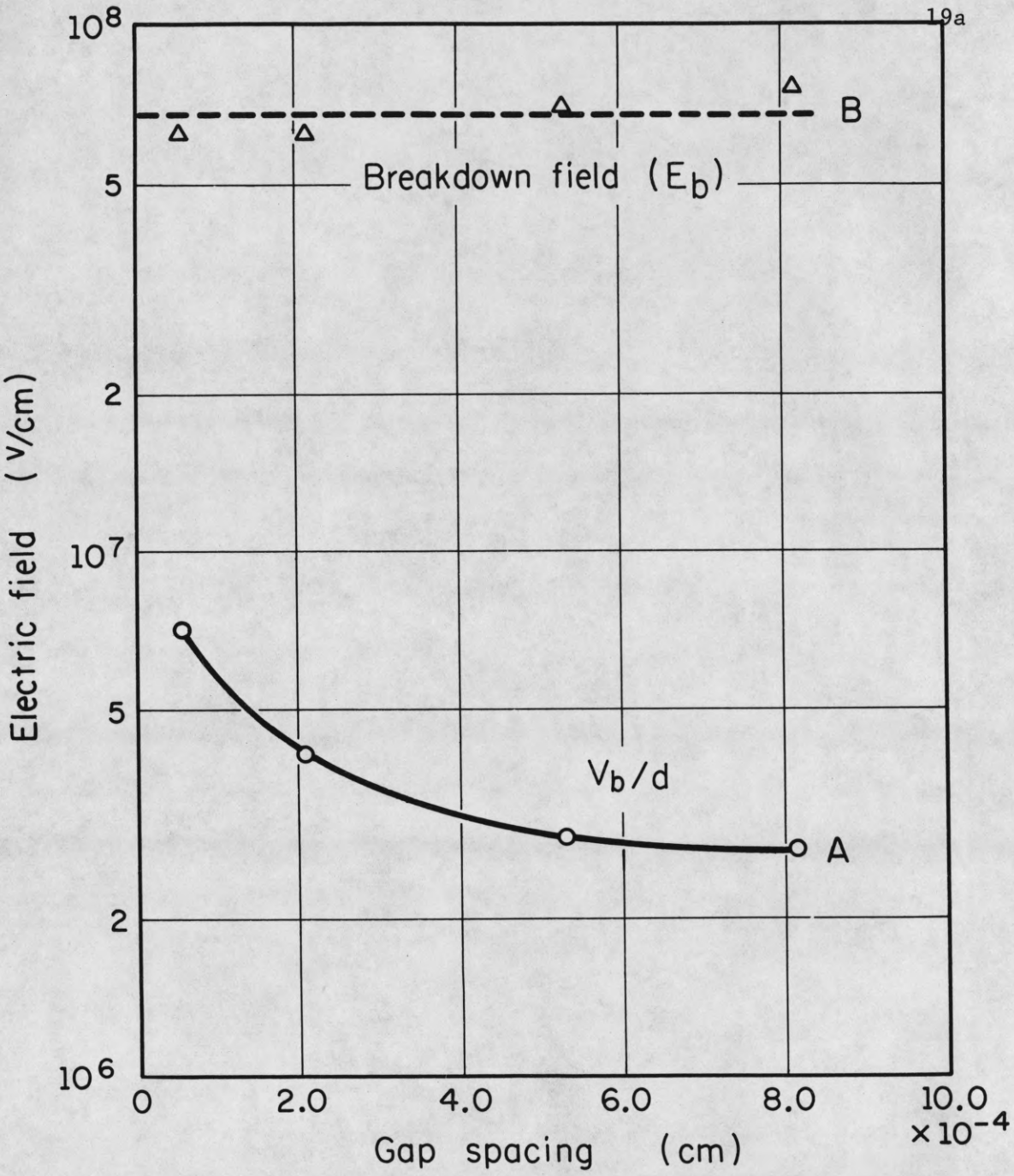

Fig. 4. Electric field at breakdown versus gap spacing from BKG data. The points on the lower curve indicate the average field at breakdown obtained by dividing the breakdown voltage, V_b, by the gap spacing, d. The upper points indicate the enhanced electric field at breakdown, obtained by multiplying the values for V_b/d from the lower curve by the corresponding measured value for ß as taken from Fig. 3. The dotted line shows the electric field at breakdown as measured by Dyke et al.

arises from a number[46] of such points or whiskers.) In this picture, breakdown occurs when the local field at a given point is raised to a critical value, the resulting current causing thermal heating and the explosion of this projection. The local field at the sharpest emitter point is determined (see section VI) from the predischarge current characteristics; hence, this picture directly relates the phenomena of initiation process to the predischarge field emission.

The success of the above picture in equating the results of Dyke and his co-workers with those of BKG seemed to us to suggest that the mechanisms for arc initiation were the same for broad area electrodes as for the point-to-plane geometry. However, the data of BKG was taken only for very small gap spacings, the maximum being about 0.001 cm. Since the region of more typical interest in electrical breakdown extends to very much larger spacings, for which a non-linear dependence of V_b on d has been observed, it was of particular interest to extend the range of observation and comparison to much larger values of d. The following experiments were undertaken to test the applicability of the above picture to larger gap spacings or to uncover evidence for the onset of a different mechanism.

IV. EXPERIMENTAL APPARATUS

The experiment was set up to study predischarge current and breakdown voltage for tungsten electrodes at gap spacings ranging from a few thousandths of a centimeter to approximately 0.5 cm and for breakdown voltages up to 250 kV. As in the BKG experiment, the gap spacings were less than the diameter of the electrodes over the entire range of values. Modern ultrahigh vacuum techniques were also used, to avoid the effects of contamination originating in the vacuum system. The electrodes could be baked to the typical bakeout temperatures (420° C) of the entire system. However, since they were held in place by stainless steel supports, it was not possible to raise the electrodes to very high temperatures to achieve atomically clean conditions at the outset of the experiment. In this important detail the experiment differed from that of BKG or of Dyke; nevertheless, it was possible to obtain reproducible results which agree very favorably with those of the above workers.

The arrangement of the electrodes and the vacuum chamber are shown in Figures 5 and 6. The evacuation was carried out in two stages. In the first stage, the vacuum chamber, with a 15 liter/sec Vacion pump and a Bayard-Alpert gauge attached, was connected to a glass oil diffusion pump. Backstreaming was limited by the use of zeolite and liquid nitrogen traps. After careful evacuation on this system (which included bakeout for 12 hours at 420°) the diffusion pump was valved off. Then the electrode vacuum chamber was baked again at this temperature while being pumped by the Vacion pump. An ultimate pressure of about 10^{-10} torr could be achieved.

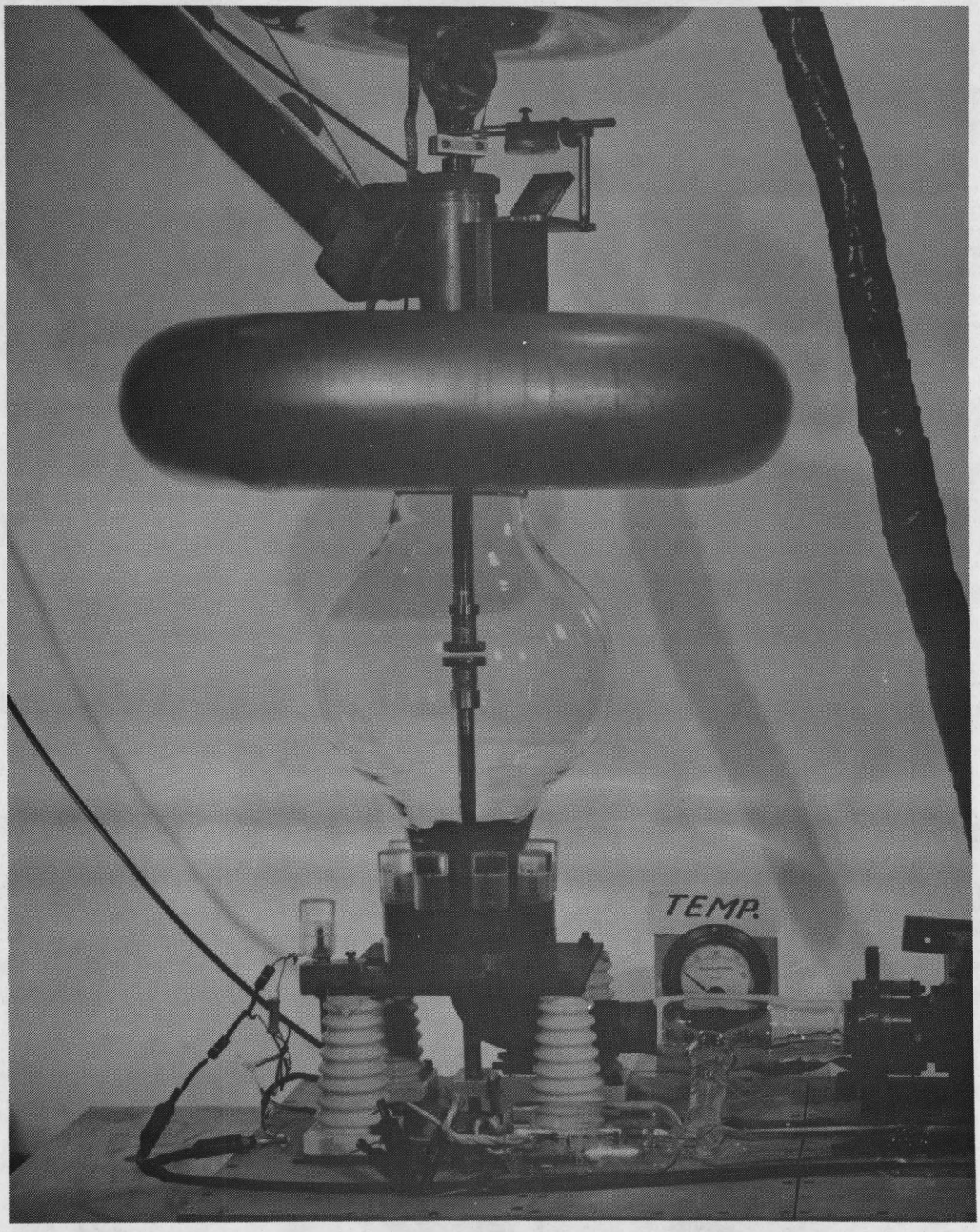

Fig. 5. Photograph of the 3.5 cm diameter tungsten electrodes in the glass vacuum chamber. High voltage is applied to the upper electrode. Field emission current is read by an electrometer attached to the bottom flange.

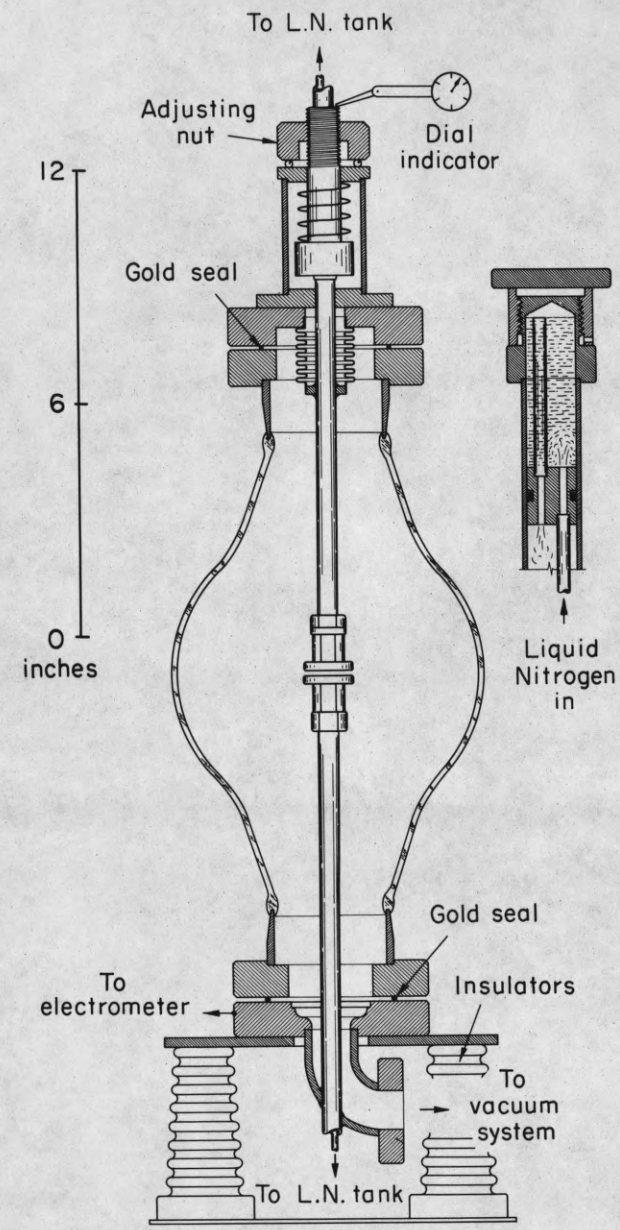

Fig. 6. Vacuum chamber assembly showing electrode cooling system and gap spacing adjustor.

The electrodes, cut from a tungsten "single crystal" boule, were machined into discs 3.5 cm in diameter and 0.7 cm thick, the edges slightly rounded to a radius of approximately 0.1 cm. The discs were vacuum-brazed to threaded molybdenum collars for attachment to the long stainless steel supports. They were then ground flat, and polished by standard mechanical techniques. Following this they were electro-polished in a solution containing 1.5% NaOH by weight in distilled water, and finally, etched in this solution to the first appearance of crystal grain boundaries. Several experiments showed that the surface treatment subsequent to the initial grinding was not critical, provided that the surfaces were clean and free of abrasive upon assembly into the vacuum system. Prior to assembling, the electrodes and vacuum chamber were scrubbed with Alconox detergent in distilled water, then repeatedly rinsed in distilled water.

Adjustment of the electrode gap spacing was made possible by attaching the upper (movable) electrode support through a flexible stainless steel bellows. The gap spacing was measured by means of a micrometer dial indicator, which indicated the displacement from a zero position denoted by the point of electrical contact. The hollow supporting stems permit circulation of fluids, allowing thermal stabilization of the electrode surfaces and the supporting structure.

To see whether the proximity of the glass chamber walls to the electrodes affects the interelectrode current or the breakdown voltage, an 8 cm diameter chamber was substituted for the 22 cm diameter chamber in a number of runs. Since no significant differences were found, it seems reasonable to conclude that the glass walls did not affect the results.

The high voltage, adjustable between 0 and 250 kV, was applied to the cathode through a 1 megohm protective resistor from an unregulated voltage doubler connected to a line voltage regulator. See Fig. 7. For values below 40 kV, both the voltage and field emission current ripple were reduced below detectability by adding a 7.5 microfarad capacitor in parallel with the power supply. For voltages above 40 kV (a range for which no smoothing capacitor was available) the meter readings, which represent the average values, must be corrected because of the nonlinear relationship between field emission current and the voltage. Capacity effects were nulled using an ac bridge, and the remaining ac components of the current and the voltage were recorded using a scope camera. These values were subsequently correlated using graphical methods to provide corrections to these average values. At peak emission currents these corrections were as much as 1.5 times the indicated dc meter values. This correction process was applied to every experimental point to obtain the true field emission current for the voltage range above 40 kV.

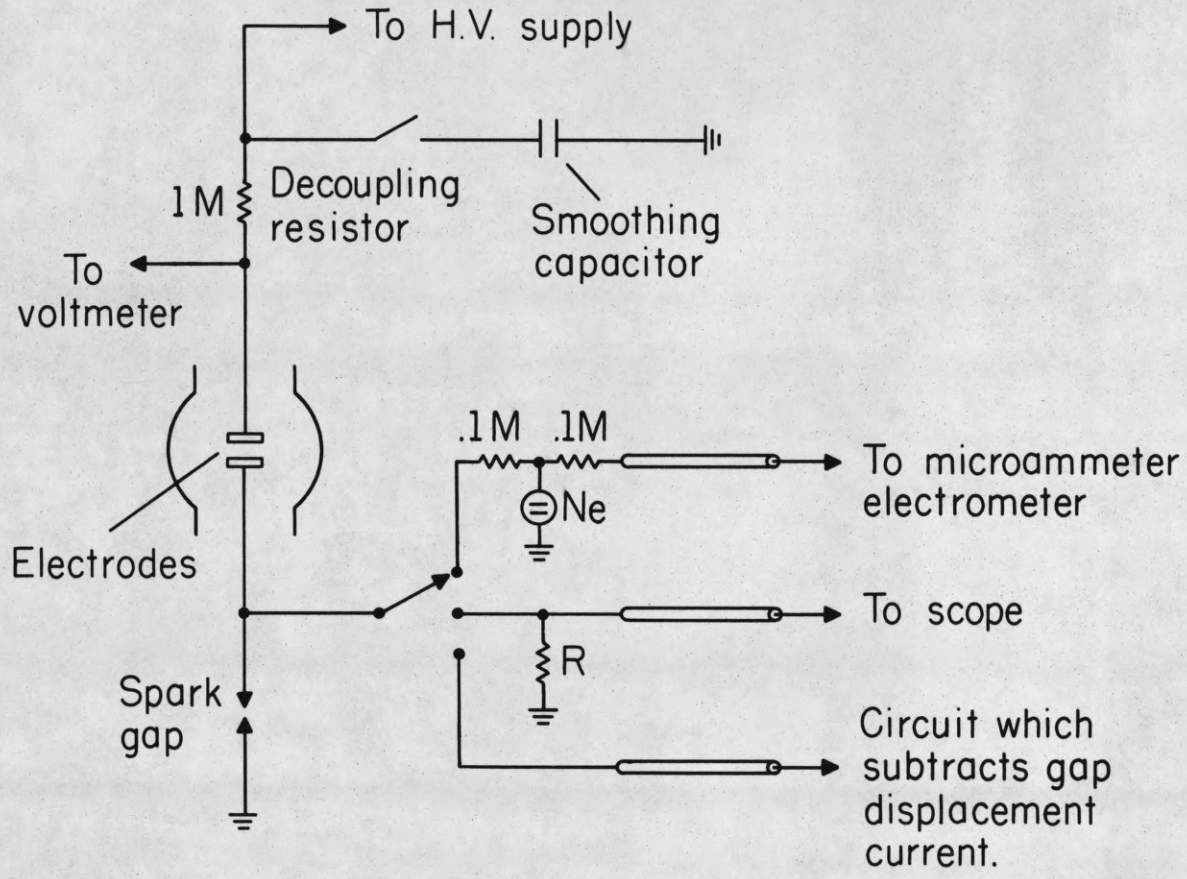

Fig. 7. Schematic circuit diagram.

V. RESULTS

A. Field emission currents

When a pair of freshly baked-out electrodes is initially exposed to high voltage, the prebreakdown current is found to fluctuate sharply. For the first few seconds, sharp spikes appear on the current wave-form, corresponding to virtual shorting of the electrodes; these are typically accompanied by gas bursts. The current pulses rapidly diminish in amplitude and increase in frequency, becoming indetectably small within 30 seconds after application of the voltage. Thereafter a continuous current is observed which is clearly attributable to field emission, as determined from its voltage dependence. The vacuum condition during most of the runs was maintained at or below 2×10^{-9} torr.

Numerous runs were taken, with different pairs of electrodes and at varying gap spacings. One of the considerations which had to be taken into account was that with continuously applied voltage, the power delivered to the anode becomes very appreciable, particularly at higher voltages. In early runs, the resulting heating of the supporting stems would cause an uncontrolled change in the gap spacing. For this reason, the electrodes and their supports were cooled with water or with liquid nitrogen during succeeding experiments; no significant changes in overall characteristics have been attributed to this cooling.

A typical run consisted of taking current readings as a function of applied voltage over a current range of several orders of magnitude. After careful measurement of the current-voltage characteristics, which were usually reproducible and reversible up to the maximum value, the voltage

was raised to the point of actual breakdown (observed as a visual flash), and its value recorded. For a given gap and voltage, the current was reproducible to about $\pm$ 10%. Data for current, I, versus applied voltage, V, were plotted in a so-called Fowler-Nordheim (F-N) plot, log I/V^2 versus $1/V$. For a better comparison of data for different gap spacings, d, the current-voltage data were sometimes presented by substituting the average field, V/d, for the potential difference, V, in the F-N plot.

Figure 8 shows the data plotted in this fashion for a typical set of runs between clean tungsten electrodes at several values of gap spacing. For a given gap, the points were taken at random for a period of several hours over the entire range of voltages below breakdown, the small spread in the data demonstrating the reproducibility with time and voltage. It will be noted that the F-N plots often (perhaps in 50% of the curves taken) exhibit a small but definite departure from a straight line at the uppermost portion of the curve in a direction of steeper slope, as is shown in the curve for d = 0.0254 cm (Curve B). This is reproducible and is believed to be a real effect, an explanation of which is given in the next section and in II.

Figure 9 shows data for a series of runs at a specified gap spacing. The difference in slope between curve A and those in the group at B, is attributed to the change in the emitting surface due to a few breakdowns which took place between runs A and B. However, it will be noted that the F-N curve is a straight line after the breakdown event as well as before. Such changes were often observed, particularly at the outset of a group of runs. However, it was also usually observed that the slope of the F-N

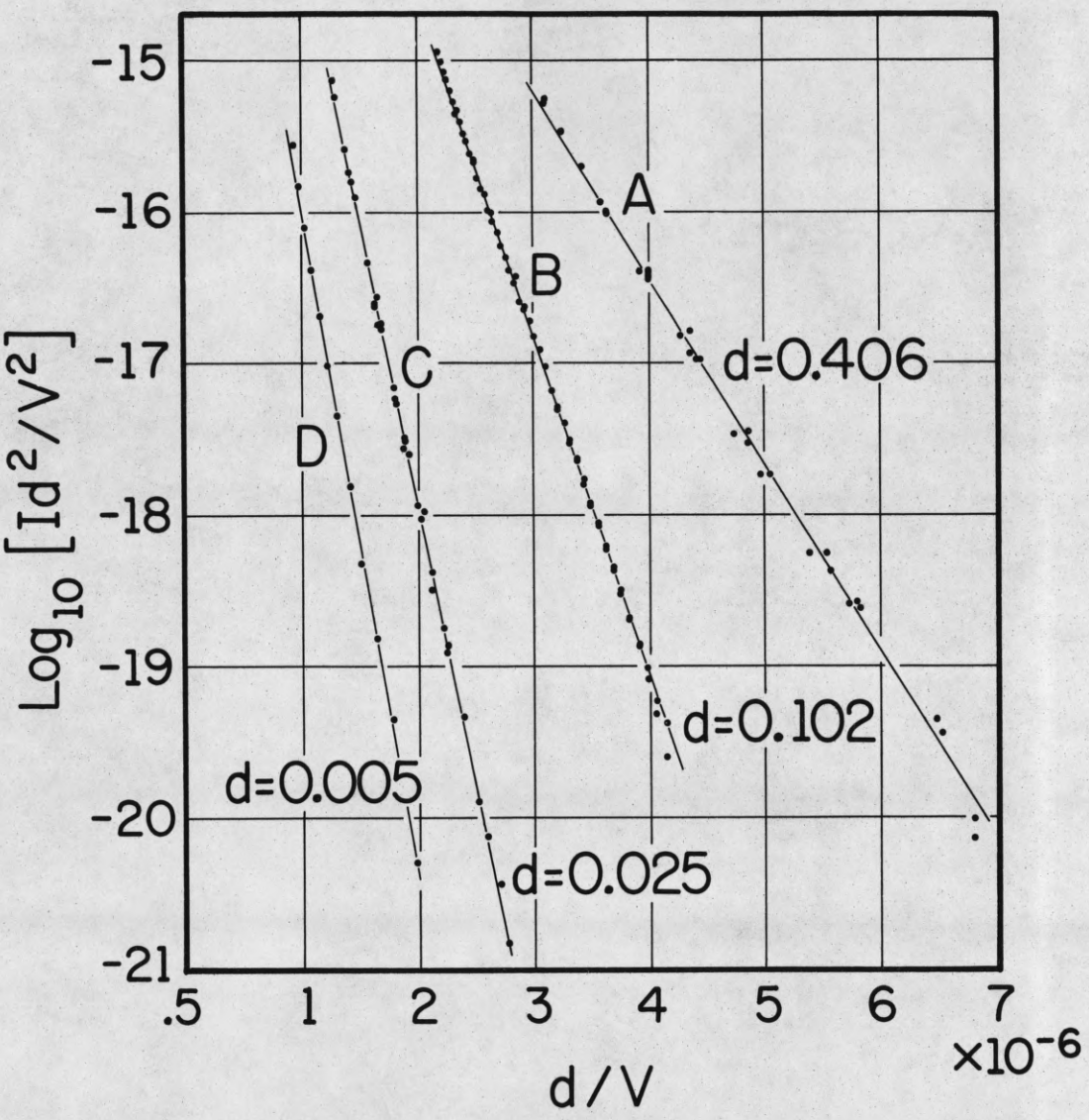

Fig. 8. Typical Fowler-Nordheim plots of the field emission current between clean parallel tungsten electrodes for various designated gap spacings (in cm).

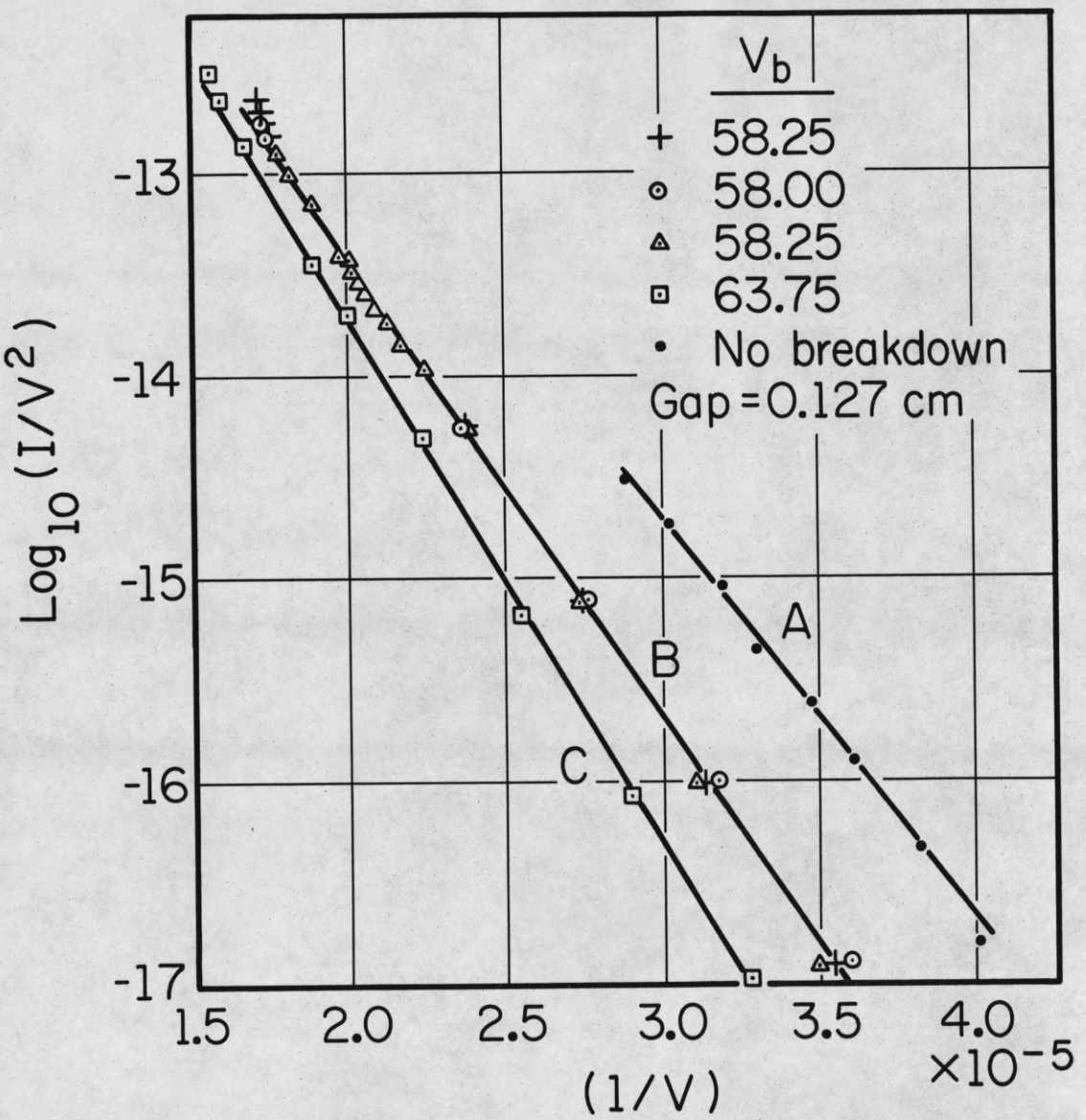

Fig. 9. Typical Fowler-Nordheim plots between successive breakdowns at a single gap spacing.

curve as well as the breakdown voltage reached a more or less stationary value after a number of successive breakdowns, as demonstrated by the runs in group B, each of which culminated in a breakdown. If the electrodes were subjected to a long period of violent sparking, a further change in slope and breakdown voltage often occurred, as shown in curve C. In addition to the above, it was observed on certain occasions that a transition from one curve to another might take place at an intermediate value of voltage and without an accompanying visible flash.

VI. DISCUSSION OF RESULTS

A. Predischarge current and critical electric field

The fact that the current-voltage data, when presented in the form of a Fowler-Nordheim plot, lie on a straight line over several orders of magnitude of the measured variables is strong evidence for attributing the conduction to field emission from the cathode. In order to interpret the data further, it is of interest to discuss the F-N curves in some detail.

The F-N equation (1) gives a relationship between the current density due to field emission from a cathode and the local electric field at its surface. The measured experimental parameters in these experiments are: total current, I ; applied voltage, V ; and the gap spacing, d. In terms of the total current, it is convenient to rewrite (1) as follows:

$$I = A\, C_1 \frac{E_s^2}{t^2(y)} \exp\left(-\frac{C_2\, \varphi^{3/2}}{E_s}\, v(y)\right) \qquad (4)$$

where A is the emitting area

C_1 and C_2 are fundamental constants

v and t are slowly varying functions of E (approximately equal to unity)

φ is the work function of the cathode material

E_s is the local electric field at the cathode surface

If the electrodes were perfectly smooth parallel infinite slabs, the electric field at the surface would be precisely given by $E_s = V/d$. However, it is

an essential assumption of this treatment that the electrodes are not ideal, i.e., that the local field at certain unspecified irregularities may be quite different from V/d. It is therefore only possible to assert that quite independent of the geometry, the electric field is proportional to the voltage, i.e.,

$$E_s = K V \quad , \tag{5}$$

where K is a proportionality constant.

If this expression is substituted in (4), it is seen that plotting $\log I/V^2$ versus 1/V should give a straight line of

$$\text{slope} = -\frac{C_2 \varphi^{3/2}}{K} s\,(y) \tag{6}$$

where s is also a slowly varying function of field (approximately unity). Thus the measured value of the slope, as taken from the experimental observations, gives directly a value of the proportionality constant if the work function of the cathode surface is known. Knowing the proportionality constant between the local electric field and the applied voltage, it is possible to determine the electric field at breakdown, E_b, from the observed value of the voltage, V_b, at which breakdown occurs.

The value of E_b has thus been determined for each of the curves of Fig. 8, using the accepted value of 4.5 eV for the average value of the work function for clean tungsten. Values of the breakdown field, E_b, for each gap spacing are listed in Table 1. Also listed are the corresponding values of the breakdown voltage, and the average field, V/d. It is seen that for these gap spacings, which range in value by two orders of

Table 1. Calculations from the curves of Fig. 8

d	V_b	E_b	V_b/d	ß	Area
cm	kV	MV/cm	MV/cm		cm^2
0.0051	5.5	64.1	1.08	59	2.8×10^{-11}
0.0254	20.8	57.5	0.816	70	3.0×10^{-10}
0.102	46.4	53.8	0.457	118	2.2×10^{-10}
0.406	135.6	70.4	0.334	211	2.8×10^{-11}

The values of breakdown voltage and breakdown field are given for four different electrode spacings. The enhancement factor, ß, is the ratio of the local field at breakdown, E_b, to the average field at breakdown, $\frac{V_b}{d}$. The emitting area is not directly measured but is computed as the ratio of the total current to the Fowler-Nordheim current density for a selected point on the F-N plot.

magnitude, the breakdown field is approximately 6×10^7 V/cm, and equal to the values obtained from the results of both BKG and of Dyke. The above values for breakdown field are plotted as a function of breakdown in Fig. 10, together with similarly obtained values from a large number of additional runs taken for gap spacings ranging from 0.005 cm to 0.635 cm. In each run, sufficient data were obtained to permit a measurement of the F-N slope (and hence, the proportionality constant) and then the voltage raised until visual breakdown occurred. For comparison, we also plot similar values of E_b as derived from the data of BKG, Gofman,[47] and Dyke et al. It is seen that for over five orders of magnitude in gap spacing, the electric field at breakdown is a constant within the experimental error of measurement at a given gap spacing, and quite independent of the geometry. The value of E_b is thus seen to be a characteristic property of the electrode material; for tungsten this value, the "critical" electric field, is equal to $6.5 \pm 1 \times 10^7$ V/cm.

A very important consequence of these results is that the value of the breakdown voltage is thus directly related to, and predictable from, the observed characteristics of the predischarge field emission currents. Knowing the critical electric field at which breakdown will occur, one can arrive in a non-destructive way at the value of voltage at which breakdown will next occur. Another important result is that under clean conditions, the breakdown characteristics for electrodes of a given material are quite independent of the geometry and, indeed, independent of whether the electrodes are single crystal or polycrystalline in structure.

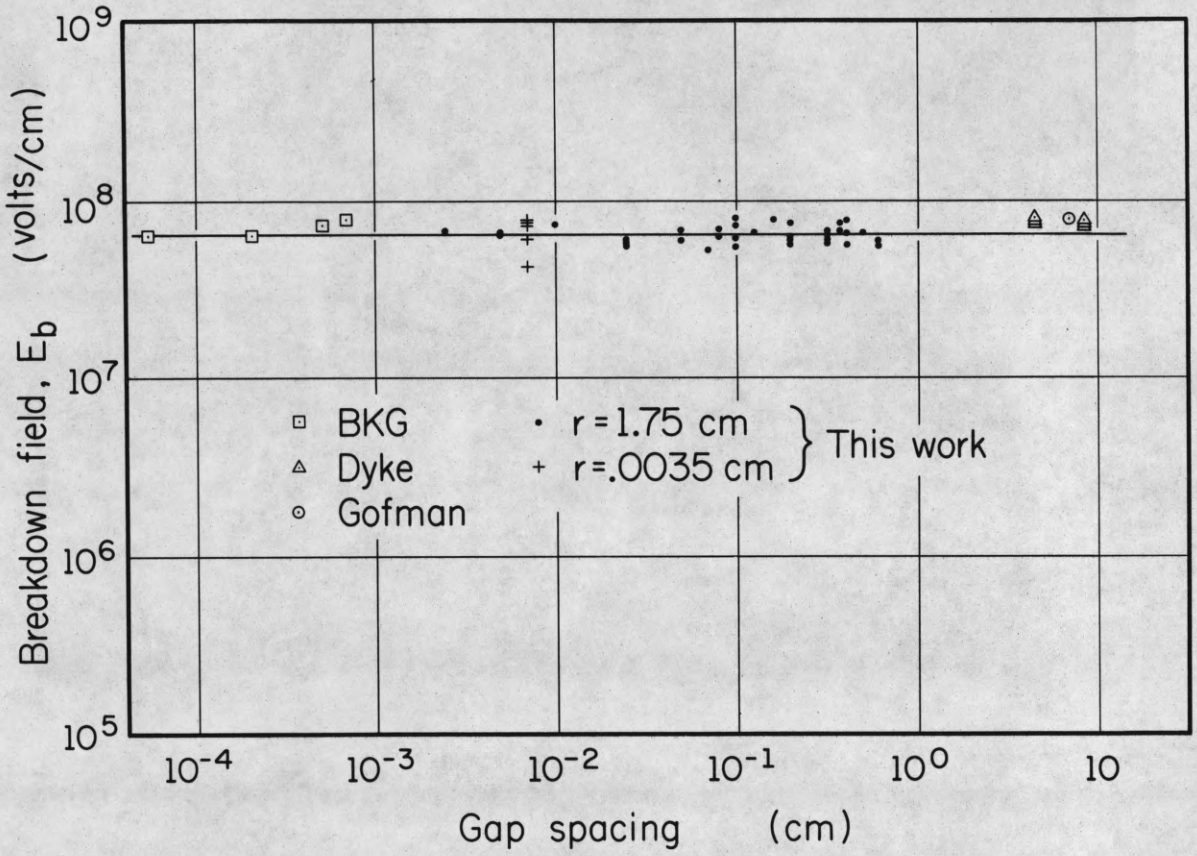

Fig. 10. Breakdown fields vs gap spacing. For each point, the breakdown field is the product of the enhancement factor ß obtained from the Fowler-Nordheim plot of prebreakdown current and the average field, V_b/d.

B. Field enhancement and the variation of breakdown voltage with gap spacing

It will be noted from Table I that the local electrical field at breakdown, E_b, varies markedly from the value of the average field as computed by dividing V_b by d. In fact, the local field at breakdown exceeds the average field in this case of parallel electrodes by a factor which BKG call the enhancement factor, ß, and which varies from values of about 50 for the smallest gap in Table I to about 200. It should be observed that ß can be directly measured from an F-N plot, since equation (5) may be rewritten

$$E_s = \beta V/d \quad . \qquad (7)$$

That is, the proportionality constant K has here been replaced by the quantity ß/d. For parallel plate geometry in which the gap spacing is small compared to the electrode dimensions, the average field is given by V/d, and ß thus represents the factor by which the average field is enhanced at the cathode surface. Thus it can be seen that when the F-N curve is plotted as in Figure 8, the slope of the curves gives ß directly.

The proportionality constant $K = \beta/d$ will be seen to have the dimensions of inverse distance. It has under some circumstances been useful to define a quantity $d_{eff} = 1/K = d/\beta$, which must still be considered to be a constant of proportionality which relates the local electric field at a selected point on the cathode to the applied voltage V. From the discussion above, it can be seen that d_{eff} could be defined as the distance between a pair of perfectly smooth parallel electrodes across which the applied voltage, V_b, would give the breakdown field. In actual situations

for plane parallel geometry, the d_{eff} may differ from d by over two orders of magnitude. It is obviously possible to obtain a d_{eff} even for a point-to-plane geometry, in which case it may be less than the measured gap spacing by over five orders of magnitude.

To compare the results of this investigation with that of other investigators, it is of interest to show the variation of breakdown voltage with gap spacing. This is done in Figure 11. It is seen that the measured points lie on a rather smooth curve which departs considerably from a constant field line. For comparison with our data, we include the data of BKG, which joins very well with ours. The combined data lie on a curve which can be approximated by a straight line of slope 0.7; at higher values of d, the data approaches rather closely the results of other workers shown in Figure 1.

The data for V_b can be shown to fall on a straight line corresponding to the constant critical field if instead of plotting versus d, we plot V_b versus d_{eff} (d/β). This is shown in the curve on the left in Figure 11 in which the abscissa for each measured point has been divided by the enhancement factor, β, as measured from the corresponding F-N curve. It is thus seen that the variation of breakdown voltage with gap spacing can be explained on the basis of the variation of the enhancement factor with the gap spacing.

The measured values of β vs. d used in the previous analysis are shown in Fig. 12. As noted in the caption, most of the measured values of β were taken from runs resulting in breakdown, but there is no significant difference from the solid curve, taken at varying electrode spacings with

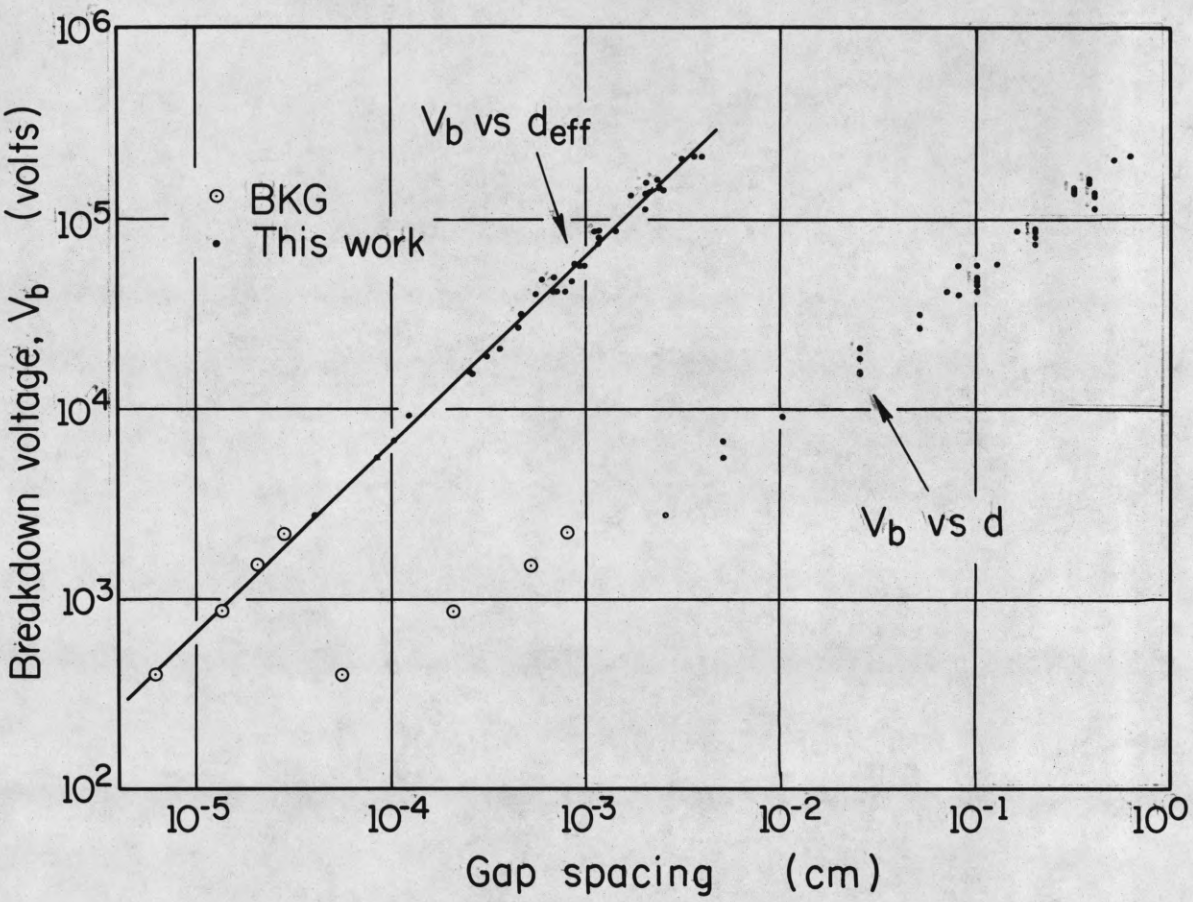

Fig. 11. Measured breakdown voltage V_b is plotted against actual gap spacing d for parallel tungsten electrodes. The points cluster about a line whose slope is 0.7. When V_b is plotted against an effective gap spacing, d_{eff}, they lie on a straight line of slope 1.0.

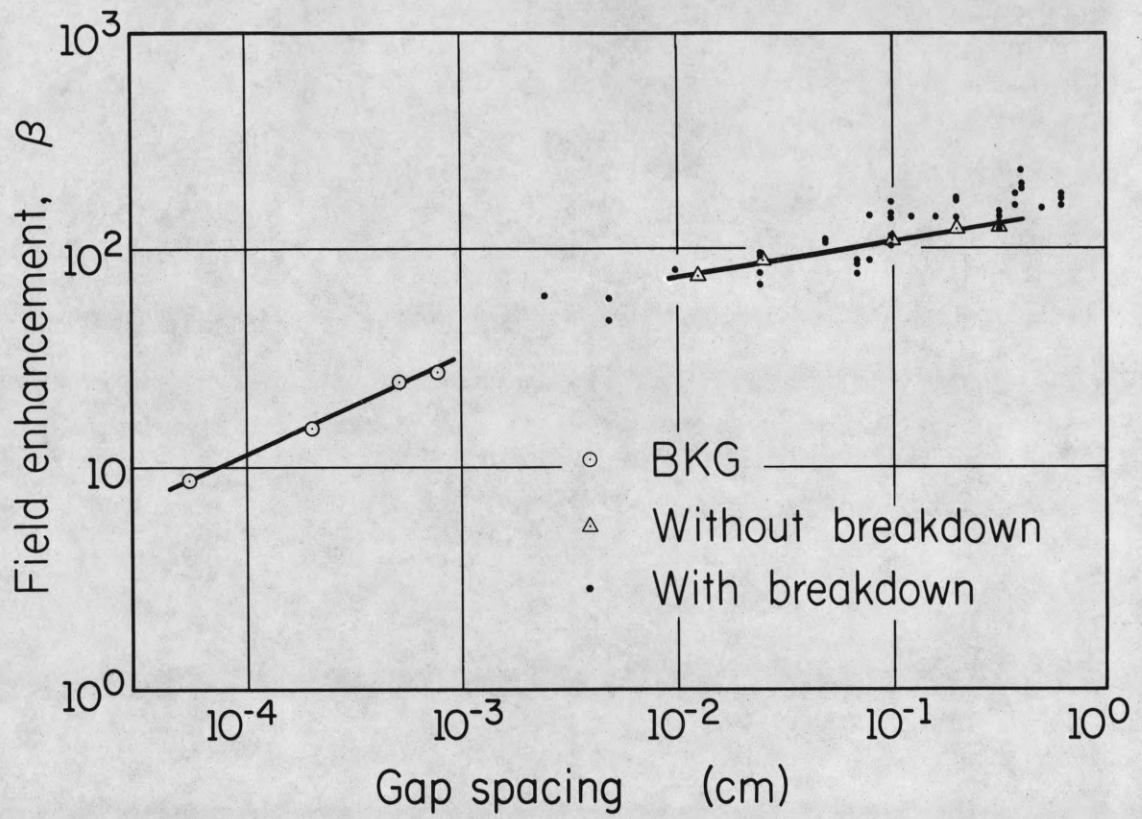

Fig. 12. Enhancement factor versus gap spacing. Values of the enhancement factor ß correspond to each breakdown point plotted in Fig. 11. The solid curves show the variation of ß with gap spacing for two sets of consecutive measurements in which no breakdown occurred. (Curve at left from BKG data).

a given electrode configuration without breakdown between measurements of β. Although the measurement of the gap spacing introduces questions and inaccuracies at very small gaps,[48] one can describe the qualitative dependence as follows. For very small gap spacings the β increases very rapidly with increasing gap spacing from unity to perhaps 40 or 50. For larger gaps, there is a rather slow variation with gap spacing, in which β rises to values of 100 or higher.

The variation of β with d can be interpreted in terms of the combined effect of an enhancement, β_1, due to microscopic projections on the cathode and a local enhancement, β_2, associated with macroscopic changes in the electric field distribution at larger gap spacings, the overall enhancement being equal to the product of these factors. For gap spacings of the order of magnitude of the height of the projections, it is reasonable to attribute the large variation in enhancement to β_1, i.e., to the variation of the microscopic fields, as proposed by BKG. It has, of course, been recognized for some time that projections on the surface of an electrode can cause the enhancement of the electric field at that point.[49,50] Smythe[51] has derived an expression for the potential surrounding a projection in the shape of a prolate hemispheroid on an otherwise smooth conducting plane. Using this derivation, we can calculate electric field at the tip of the boss and the following expression for the enhancement factor, i.e., the ratio of the maximum field to the average field is obtained.[52]

$$\beta_1 = \frac{1}{\eta\left(\coth^{-1}\eta - \frac{1}{\eta}\right)(\eta^2 - 1)}, \qquad (8)$$

where η is a geometrical factor relating to the height, c, and the base radius, b, of the projection.

$$\eta = \frac{c}{(c^2 - b^2)^{1/2}} \quad .$$

Figure 13 shows a graph of the numerically calculated β_1 factor as a function of the ratio of the height c to the base radius b. It is seen that the microscopic enhancement factor, β_1, would be expected to have values in range of those experimentally observed for ratios of height to radius between 10 and 20 for the shape here assumed as a model.

In the above derivation, the field enhancement is determined solely by the dimensions of the projection above an infinite plane, assuming that the opposite electrode is at such a large distance as to have no effect on the field at the projection and hence on β. At very small gap distances, this is clearly not the case; one can calculate the field in the vicinity of the projection to determine a critical distance at which the electric field is no longer perturbed by the opposing electrode. Within this distance, one would, in fact, expect a very rapid change on β_1 as was observed by BKG. A calculation for the hemispheroidal model indicates that the critical distance is approximately twice the height of the projection. We can thus get an indication of the size of the whiskers in the BKG experiment; since the major change in β_1 took place over a distance of about 5×10^{-4} cm, one concludes that the largest projections were of the order of half that in height, i.e., a few wave-lengths of visible light. If one makes the reasonable assumption that the point emits electrons from a small area at the very

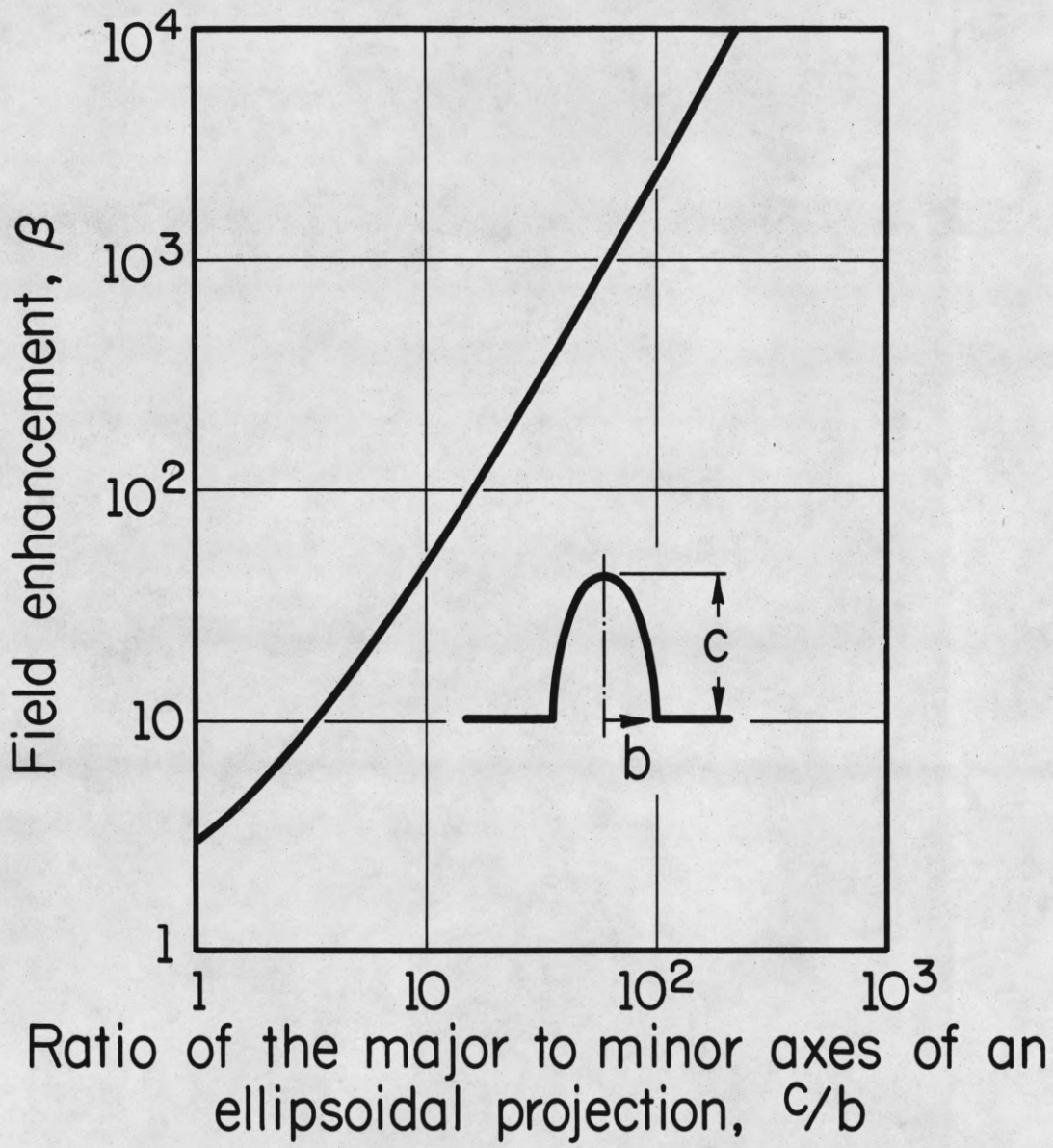

Fig. 13. Microscopic field enhancement factor β_1 as a function of the geometry for an ellipsoidal boss on an otherwise flat infinite plane.

tip (a few percent of the base area), the values for the emitting area as derived from the Fowler-Nordheim curves give a self-consistent picture of the approximate shape[53] for the points.

For large values of gap spacing, the β_1 reaches an asymptotic value. Since the data of Figure 12 clearly demonstrate a variation of β with d which must be associated with macroscopic enhancement at large gap spacings and not to a change in the microstructure at the cathode, it seems reasonable to attribute this effect to field enhancement at the edges of the electrodes. Calculations[54] using as a model a pair of semi-infinite slab electrodes with rounded corners, indicate that when the gap spacing becomes large compared to the radius of curvature at the edges of the electrodes, the enhancement factor, β_2, may be appreciable. The results of these calculations are shown in Figure 14.

Although this calculation is at best an approximation to the actual configuration, the observed variation of β at large gap spacings is consistent with this analysis. Though questions inevitably remain with respect to the details of the physical nature of the projections, especially insofar as their configuration and surface condition may vary, it seems reasonable to attribute the principal features of the variation of breakdown voltage with gap spacing to the dependence of field enhancement on the gap spacing over the range of voltages covered in these experiments.

C. Multiple points on broad electrodes

As previously noted, BKG came to the conclusion that the emission must arise predominantly from a single point projection since their data

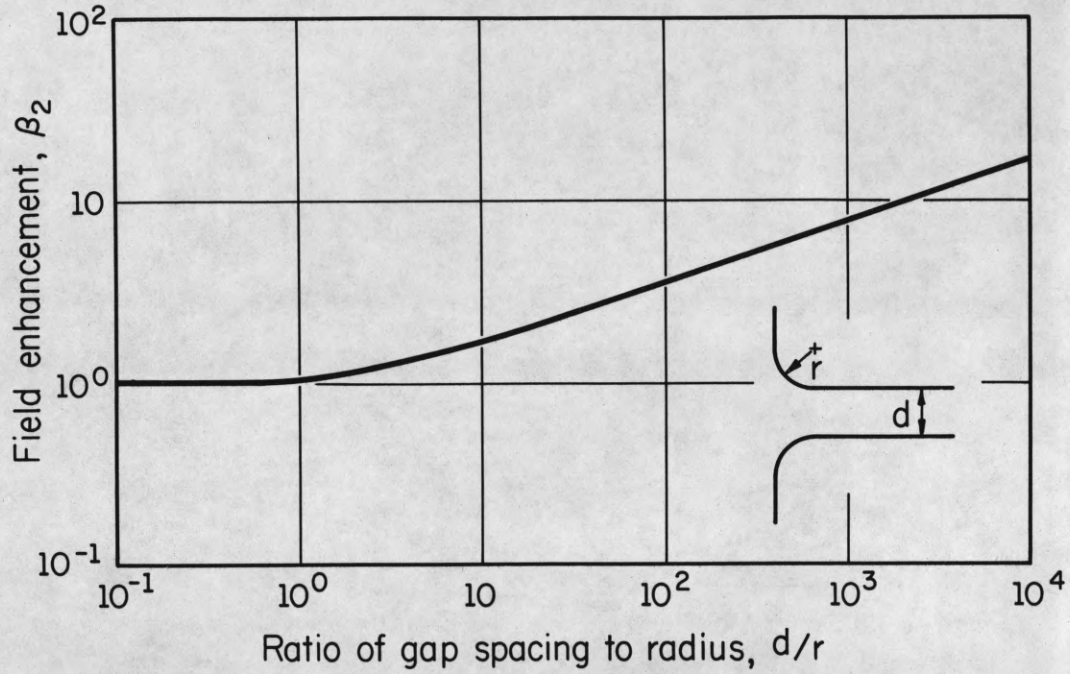

Fig. 14. Enhancement factor β_2 vs d/r. The curve presents the ratio of the maximum value of the electric field in the region of the rounded portion of the slab electrode to the electric field inside the gap. The solution was obtained by Schwarz-Christoffel transform methods.

appeared as single straight line on an F-N plot. Their argument, of course, is based on the premise that if two (or more) projections with different ß's were involved, one would expect a non-linear curve to result. However, although the F-N plots for our data for many runs are also straight lines (as shown in Figs. 8 and 9) there was strong experimental evidence that the emission arises from multiple points. One piece of evidence is inherent in the nature of successive curves in Figure 9; after a few initial runs, it was typical to find that several succeeding runs would be virtually indistinguishable. While this is readily explained on the basis of many more or less similar projections, only one of which is destroyed in the breakdown process, it is quite difficult to visualize a situation in which a single point dominates the entire emission, then is destroyed and somehow replaced by an identical point at another location.

A second form of experimental evidence for multiple points arose from visual observations of the electrodes during the course of a given run. When the predischarge electrode current reaches a value of the order of a microampere, there begin to appear sharply defined blue-green pin-points of light at the surface of the anode. The light is quite faint and requires dark adaptation to be observed. The brightness of the spots increases with increasing current, and they number from about 1 to 10 per cm^2. For an electrode spacing of about 0.4 cm (V = 160 kV, I - 150 μA), their diameter is approximately 0.01 cm. Although the spot pattern is relatively unvarying over a period of time (at constant voltage and current), certain spots may disappear and new spots appear elsewhere from time to time either with or without visible breakdown, the total number remaining roughly constant.

However, one or more spots are always seen to disappear in conjunction with a visible breakdown.

The variation of light intensity with current clearly associates the many spots of light with electrons impinging on the anode, while their even distribution over the entire anode seems to rule out the possibility that they are caused by electrons from a single point. As a matter of fact, a straightforward application of calculations on the spreading of an electron beam from a whisker of the dimensions postulated in section VI B indicates that one would expect the electron beam from a single whisker to have a diameter of about 0.01 cm by the time it strikes the anode at the above spacing. Thus, it seems plausible to attribute each individual spot to the beam from an individual whisker or protrusion at the cathode. This interpretation is supported by the observation that a lateral movement of the cathode with respect to the anode (maintaining a constant gap spacing) caused the entire pattern of spots to move across the anode in conjunction with the cathode motion.

The association of the field emission from extended electrodes with multiple emission sites has also been demonstrated by Little and Whitney[55] and by Brodie and Weissman.[56] Singer and Doolittle[57] observed point sources of x-rays arising from extended electrodes. A suggestion as to the possible origin of the visible light spots comes from a study by E. Silverman,[58] who attributes a blue-green spot on a copper target bombarded by a 25 kV electron beam to bremsstrahlung. Preliminary calculations appear to support the plausibility of this explanation.

Although questions may remain with respect to the detailed mechanisms responsible for the visible spots of light, the above observations

leave little doubt as to the multiple source origin of the predischarge field emission current, and hence reopen the question of the BKG interpretation of the Fowler-Nordheim plots. These considerations motivated a very extensive study of the formation and role of whiskers in the predischarge and initiation processes, the results of which are presented in II. For the present, it should suffice to report that additional direct evidence has been adduced for the existence of multiple whiskers or points as sources of field emission at the cathode. Furthermore, a numerical analysis of the shape of the curve to be expected from a reasonable distribution of points of different ß's shows that a straight line may indeed be expected from such an array. Under some circumstances, a wider distribution of point shapes may result in departures from linearity, and the departures at high currents (such as that in curve B of figure 8 in the direction of a steeper slope (smaller ß's) are attributed to such an effect. It is important to note that the values listed in Table I were calculated from the straight portion of the curve, attributable to the sharper points. As was typical in such cases, this portion of the curve resulted in a value of E_b in agreement with data from curves which did not depart from linearity.

The spontaneous change in the distribution of spots referred to above suggests an explanation of other experimental observations. In some cases, such a change has been associated with the transition from one F-N curve to another described in section V. This transition then represents a change in the structure of the cathode or possibly of the anode in which material may be transferred between the electrodes at voltages below the range of electrical breakdown. The disappearance of a spot on the cathode

may be due to the explosion of one of the whiskers, the resulting discharge being quenched before a visible flash is formed. Thus the description of the initiation process in terms of enhanced field emission from multiple whiskers provides in addition an explanation of a number of observations of predischarge phenomena. A more detailed discussion is contained in II.

VII. SUMMARY DISCUSSION

A review of a large number of experimental measurements on the initiation of electrical breakdown has been carried out, and several theories for this process have been subjected to critical study. Experiments have been carried out which have extended the available data on electrical breakdown between refractory metal electrodes under ultrahigh vacuum conditions. These have been interpreted on the basis of a single picture which explains and relates the phenomena of predischarge currents and the initiation of breakdown. It is shown that both predischarge conduction and breakdown can be attributed to the existence of fine microscopic points or whiskers; furthermore, the field emission from the points can be used as a tool to ascertain the approximate geometry of and field enhancement due to such whiskers in a non-destructive manner and thus to predict the voltage at which the breakdown will next occur. The picture also explains the anomalous dependence of predischarge currents and breakdown voltage on gap spacing. When analysed on this basis, the observations of at least four major experiments utilizing clean tungsten electrodes in a wide variety of electrode geometries, have been shown to give completely consistent agreement, within the experimental error. Their results give strong support to a principal conclusion of this study: that breakdown occurs when the local electric field at microscopic projections on the cathode reaches a critical value, independent of the geometry or gap spacing.

Preliminary measurements of predischarge currents and electrical breakdown for electrodes of other materials[59] have been made, giving rather similar though less reproducible results; such studies are part of a continuing program.

The results herein described formed the motivation and starting point for a detailed study of the projections on electrodes and their effect on electrical breakdown in vacuum. These studies, which included the development and use of techniques for the direct observation of the whiskers are described in II.

ACKNOWLEDGMENTS

The authors gratefully acknowledge the contribution to this experiment of T. C. Casale and F. K. Konrad who were instrumental in the development of the apparatus and the techniques.

[1]R. F. Earhard, Phil. Mag. 1, 147 (1901) and G. M. Hobbs, Phil Mag. 10, 617 (1905) studied gas breakdown at very small gap spacings (of the order of a few wave-lengths of light). They discovered that breakdown occurred at voltages much lower than the minimum gas breakdown potential and was independent of the gas composition. Hobbs noted that breakdown occurred at a constant value of electric field, roughly 10^6 V/cm and depended on the electrode material. Although these experiments were performed at high pressures (above 10 torr), the mean free paths for electrons and gases were comparable to or greater than the dimensions of the gap and hence the conditions of electrical breakdown in high vacuum prevailed.

[2]R. A. Millikan and R. A. Sawyer, Phys. Rev. 12, 167 (1918).

[3]Quoting from the above paper: "(sparking potentials)....were found to show interesting fatigue effects, the initial discharge potential rising from, say 300,000 V/cm to 1,000,000 V/cm with continued sparking, as though the sparking potential depended on the surface condition. After the sparking potentials had been increased from say 300 000 V/cm to 1 200 000 V/cm, if the electrodes were allowed to stand, the spark potential would fall in the course of twenty-four hours to about the initial value. Reversal of the electrodes would also produce a large change in the spark potential..."

[4]A. S. Denholm, Can. J. Phys. 36, 476 (1958).

[5]J. G. Trump, J. Appl. Phys. 18, 327 (1947).

[6]I. N. Slivkov, Soviet Phys.-Tech. Phys. 2, 9 (1958).

[7]H. W. Anderson, Elec. Eng. 54, 1315 (1935).

[8]J. L. McKibbon and R. K. Beauchamp, AECD-2039 (1948).

[9]L. I. Pivovar, V. I. Gordienko, and V. M. Tubaev, Soviet Phys.-Tech. Phys. 3, 2101 (1958).

[10]W. Parkins, AEC-MDDC-858 (1947).

[11]O. E. Myers, AEC-LRL-158 (1955).

[12]N. B. Rosanova and V. T. Granovskii, Soviet Phys.-Tech. Phys. 1, 471 (1956).

[13]H. Heard, AEC-UCRL-2252 (1953).

[14]W. S. Boyle, P. Kisliuk, and L. H. Germer, J. Appl. Phys. 26, 720 (1955).

[15]H. W. Anderson, Elec. Eng, 54, 1315 (1935).

[16]E. W. Müller, Z. Physik 102, 734 (1936).

[17]D. Alpert, J. Appl. Phys. 24, 860 (1953), and J. Appl. Phys. 25, 202 (1954).

[18]W. P. Dyke and J. K. Trolan, Phys. Rev. 89, 799 (1953).

[19]W. P. Dyke, J. K. Trolan, E. E. Martin, and J. P. Barbour, Phys. Rev. 91, 1043 (1953).

[20]W. W. Dolan, W. P. Dyke, and J. K. Trolan, Phys. Rev. 91, 1054 (1953).

[21]A. J. Ahearn, Phys. Rev. 50, 238 (1936).

[22]R. H. Fowler and L. Nordheim, Proc. Roy. Soc. (London) A119, 173 (1928).

[23]L. Nordheim, Proc. Roy. Soc. (London) A121, 626 (1928).

[24]For a detailed presentation of the theory of field emission, see R. H. Good, Jr. and E. W. Muller, Handbuch der Physik 21, 176 (1956).

[25]This technique was first used by R. Haefer, Z. Physik 120, 261, 270 (1940).

[26]See, for example, P. F. Browne, Proc. Phys. Soc. B68, 564 (1955), and H. W. Anderson[(15)].

[27]L. C. Van Atta and R. J. Van de Graaff, Phys. Rev. 43, 158 (1933).

[28]R. Arnal, Ann. Physik 12, 830 (1955), in French; USAEC-TR-2837, English translation.

[29]W. K. Mansfield and R. Fortescue, Brit. J. Appl. Phys. 8, 73 (1957).

[30]J. Murray, UCRL Report 9506 (Sept., 1960) and F. Rohrback and C. Germain (CERN, private communication).

[31]L. I. Pivovar and V. I. Gordienko, Soviet Phys.-Tech. Phys. 7, 908 (1963).

[32]J. G. Trump and R. J. Van de Graaff, J. Appl. Phys. 18, 327 (1947).

[33]B. Aarset, R. W. Cloud, and J. G. Trump, J. Appl. Phys. 25, 1365 (1954).

[34]A. I. Bennett, J. Appl. Phys. 28, 1251 (1957).

[35]L. T. Leland, R. Olsen, AEC-LA-2344 (1960).

[36]M. Raether, CSL Report R-148 (July, 1962).

[37]L. Cranberg, J. Appl. Phys. 23, 518 (1952).

[38]I. N. Slivkov, Soviet Phys.-Tech. Phys. 2, 1928 (1958).

[39]D. Alpert and D. Lee, CSL Report R-129 (June, 1962).

[40]H. Heard and E. Lauer, AEC-UCRL-2051 (1953).

[41]W. H. Bennett, Phys. Rev. 45, 890 (1934).

[42]W. S. Boyle, P. Kisliuk, and L. H. Germer, J. Appl. Phys. 26, 720 (1955).

[43]A. Maitland, J. Appl. Phys. 32, 2399 (1961).

[44]G. E. Vibrans, Lincoln Lab. Technical Report 308 (18 April, 1963).

[45]This work was first described in CSL Report R-129 and later given as a paper: D. Alpert, D. A. Lee, E. M. Lyman, and H. E. Tomaschke, Bull. Am. Phys. Soc. 9, 181 (1964).

[46]For a discussion and references to other authors, see section VI C.

[47]I. I. Gofman, O. D. Protopopov, and G. N. Shuppe, Soviet Phys.-Solid State 2, 1203 (1961). These data are the results of a most recently published careful study of field emission and breakdown taken with point-to-plane geometry similar to that of Dyke et al.

[48]For example, it is significant to note that zero gap spacing is determined in these measurements by the point of electrical contact and hence,

for BKG, the gap spacing is defined as the distance from the tip of the largest projection to the opposite electrode.

[49]W. Schottky, Z. Physik 14, 63 (1923).

[50]T. J. Lewis, J. Appl. Phys. 26, 1405 (1955).

[51]W. R. Smythe, Static and Dynamic Electricity (McGraw-Hill Book Co., Inc., New York, 1950), 2nd ed., p. 168.

[52]H. Tomaschke, Thesis, A study of the projections on electrodes and their effect on electrical breakdown in vacuum, Univ. of Illinois, 1964.

[53]As will be shown in II. these considerations are given further confirmation by the direct observation of whiskers on tungsten electrode surfaces taken with the electron microscope.

[54]D. Lee, CSL Report R-230 (September, 1964).

[55]R. P. Little and W. T. Whitney, NRL Report No. 5944 (May 20, 1963) and J. Appl. Phys. 34, 2430 (1963).

[56]I. Brodie and I. Weissman, Vacuum, to be published.

[57]B. Singer and H. Doolittle (Private communication).

[58]E. Silverman, Lincoln Laboratory, MIT, High Power Tube Program Semiannual Report (Dec., 1962).

[59]I. Brodie has shown that similar conclusions are applicable for pure nickel electrodes. J. Appl. Phys. 35, 2324 (1964).

Distribution list as of February 1, 1964

1 Director
Air University Library
Maxwell Air Force Base, Alabama
Attn: CR-4803a

1 Redstone Scientific Information Center
U.S. Army Missile Command
Redstone Arsenal, Alabama

1 Electronics Research Laboratory (Unclassified)
University of California
Berkeley 4, California

2 Hughes Aircraft Company
Florence and Teale
Culver City, California
Attn: N. E. Devereux
Technical Document Center

3 Autonetics (Unclassified)
9150 East Imperial Highway
Downey, California
Attn: Tech. Library, 3041-11

1 Dr. Arnold T. Nordsieck
General Motors Corporation
Defense Research Laboratories
6767 Hollister Avenue
Goleta, California

1 University of California (Unclassified)
Lawrence Radiation Laboratory
P. O. Box 808
Livermore, California

1 Mr. Thomas L. Hartwick
Aerospace Corporation
P. O. Box 95085
Los Angeles 45, California

1 Lt. Colonel Willard Levin
Aerospace Corporation
P. O. Box 95085
Los Angeles 45, California

1 Professor Zorab Kaprelian
University of Southern California
University Park
Los Angeles 7, California

1 Sylvania Electronic Systems - West
Electronic Defense Laboratories
P. O. Box 205
Mountain View, California
Attn: Documents Center

1 Varian Associates
611 Hansen Way
Palo Alto, California
Attn: Dr. Ira Weissman

1 Huston Denslow (Unclassified)
Library Supervisor
Jet Propulsion Laboratory
California Institute of Technology
Pasadena, California

1 Professor Nicholas George
California Institute of Technology
Electrical Engineering Department
Pasadena, California

1 Space Technology Labs., Inc.
One Space Park
Redondo Beach, California
Attn: Acquisitions Group
STL Technical Library

2 Commanding Officer and Director
U.S. Naval Electronics Laboratory
San Diego 52, California
Attn: Code 2800, C. S. Manning

1 Commanding Officer and Director
U.S. Navy Electronics Laboratory
San Diego 52, California
Attn: Library

1 Office of Naval Research Branch Office
1000 Geary Street
San Francisco, California

1 The RAND Corporation
1700 Main Street
Santa Monica, California
Attn: Library

1 Stanford Electronics Laboratories (Unclassified)
Stanford University
Stanford, California
Attn: SEL Documents Librarian

1 Dr. L. F. Carter
Chief Scientist Air Force
Room 4E-324, Pentagon
Washington 25, D. C.

1 Mr. Robert L. Feik
Associate Director for Research
Research and Technology Division
AFSC
Bolling Air Force Base 25, D. C.

1 Captain Paul Johnson (USN-Ret)
National Aeronautics and Space
Administration
1520 H Street, N. W.
Washington 25, D. C.

1 Major Edwin M. Myers
Headquarters USAF (AFRDR)
Washington 25, D. C.

1 Dr. James Ward
Office of Deputy Director
(Research and Info)
Department of Defense
Washington 25, D. C.

1 Dr. Alan T. Waterman
Director, National Science Foundation
Washington 25, D. C.

1 Mr. G. D. Watson
Defense Research Member
Canadian Joint Staff
2450 Massachusetts Ave., N. W.
Washington 8, D. C.

1 Mr. Arthur G. Wimer
Chief Scientist
Air Force Systems Command
Andrews Air Force Base
Washington 25, D. C.

1 Director, Advanced Research
Projects Agency
Washington 25, D. C.

1 Air Force Office of Scientific Branch
Directorate of Engineering Sciences
Washington 25, D. C.
Attn: Electronics Division

1 Director of Science and Technology
Headquarters, USAF
Washington 25, D. C.
Attn: AFRST-EL/GU

1 AFRST - SC
Headquarters, USAF
Washington 25, D. C.

1 Headquarters, R & T Division (Unclassified)
Bolling Air Force Base
Washington 25, D. C.
Attn: RTHR

1 Headquarters, U. S. Army Material Command
Research Division, R & D Directorate
Washington 25, D. C.
Attn: Physics & Electronics Branch
Electronics Section

1 Commanding Officer
Diamond Ordnance Fuze Laboratories
Washington 25, D. C.
Attn: Librarian, Room 211, Bldg. 92

1 Operation Evaluation Group
Chief of Naval Operations (OP-03EG)
Department of Navy
Washington, D. C. 20350

1 Chief of Naval Operations (Code OP-ONT)
Department of the Navy
Washington, D. C. 20350

1 Commanding Officer
U. S. Army Personnel Research Office
Washington 25, D. C.

1 Commanding Officer & Director
Code 142 Library
David W. Taylor Model Basin
Washington, D. C. 20007

1 Chief, Bureau of Ships (Code 686)
Department of the Navy
Washington, D. C. 20360

1 Chief, Bureau of Ships (Code 732)
Department of the Navy
Washington, D. C. 20360

1 Chief, Bureau of Naval Weapons
Technical Library, DLI-3
Department of the Navy
Washington, D. C. 20360

1 Director, (Code 5140)
U. S. Naval Research Laboratory
Washington, D. C. 20390

1 Chief of Naval Research (Code 437)
Department of the Navy
Washington, D. C. 20360

1 Dr. H. Wallace Sinaiko (Unclassified)
Institute for Defense Analyses
Research & Engineering Support Division
1666 Connecticut Ave., N. W.
Washington 9, D. C.

1 Data Processing Systems Division
National Bureau of Standards
Conn. at Van Ness
Room 239, Bldg. 10
Washington 25, D. C.
Attn: A. K. Smilow

1 National Bureau of Standards (Unclassified)
Research Information Center &
Advisory Service on Information
Processing
Data Processing Systems Division
Washington 25, D. C.

1 Exchange and Gift Division (Unclassified)
The Library of Congress
Washington 25, D. C.

1 NASA Headquarters
Office of Applications
400 Maryland Avenue, S. W.
Washington 25, D. C.
Attn: Mr. A. M. Greg Andrus
Code FC

1 APGC (PGAPI)
Eglin Air Force Base
Florida

1 Martin Company
P. O. Box 5837
Orlando, Florida
Attn: Engineering Library
MP-30

1 Commanding Officer
Office of Naval Research, Chicago Branch
6th Floor, 230 North Michigan
Chicago 1, Illinois

1 Laboratories for Applied Sciences
University of Chicago
6220 South Drexel
Chicago 37, Illinois

1 Librarian (Unclassified)
School of Electrical Engineering
Purdue University
Lafayette, Indiana

1 Donald L. Epley (Unclassified)
Department of Electrical Engineering
State University of Iowa
Iowa City, Iowa

1 Commanding Officer
U. S. Army Medical Research Laboratory
Fort Knox, Kentucky

2 Keats A. Pullen, Jr.
Ballistic Research Laboratories
Aberdeen Proving Ground, Maryland

1 Director
U. S. Army Human Engineering Laboratories
Aberdeen Proving Ground, Maryland

1 Mr. James Tippett
National Security Agency
Fort Meade, Maryland

1 Commander
Air Force Cambridge Research Laboratories
Laurence G. Hanscom Field
Bedford, Massachusetts

1 Dr. Lloyd Hollingsworth
Director, ERD
AFCRL
L. G. Hanscom Field
Bedford, Massachusetts

1 Data Sciences Laboratory
Air Force Cambridge Research Lab
Office of Aerospace Research, USAF
L. G. Hanscom Field
Bedford, Massachusetts
Attn: Lt. Stephen J. Kahne - CRB

1 Instrumentation Laboratory (Unclassified)
Massachusetts Institute of Technology
68 Albany Street
Cambridge 39, Massachusetts

1 Research Laboratory of Electronics (Unclassifi
Massachusetts Institute of Technology
Cambridge 39, Massachusetts
Attn: Document Room 26-327

1 Dr. Robert Kingston
Lincoln Laboratories
Lexington, Massachusetts

1 Lincoln Laboratory (Unclassified)
Massachusetts Institute of Technology
P. O. Box 73
Lexington 73, Massachusetts
Attn: Library, A-082

1 Sylvania Electric Products, Inc.
Electronic Systems
Waltham Labs. Library
100 First Avenue
Waltham 54, Massachusetts

1 Minneapolis-Honeywell Regulator Co.
Aeronautical Division (Unclassified)
2600 Ridgeway Road
Minneapolis 13, Minnesota
Attn: Dr. D. F. Elwell
Main Station: 625

1 Inspector of Naval Material
Bureau of Ships Technical Representative
1902 West Minnehaha Avenue
St. Paul 4, Minnesota

20 Activity Supply Officer, USAELRDL
Building 2504, Charles Wood Area
Fort Monmouth, New Jersey
For: Accountable Property Officer
Marked: For Inst. for Exploratory Research
Inspect at Destination
Order No. 576-PM-63-91

1 Commanding General
U. S. Army Electronic Command
Fort Monmouth, New Jersey
Attn: AMSEL-RE

1 Mr. A. A. Lundstrom
Bell Telephone Laboratories
Room 2E-127
Whippany Road
Whippany, New Jersey

1 AFMDC (MDSGP/Capt. Wright)
Holloman Air Force Base
New Mexico

1 Commanding General
White Sands Missile Range
New Mexico

1 Microwave Research Institute
Polytechnic Institute of Brooklyn
55 John Street (Unclassified)
Brooklyn 1, New York

1 Cornell Aeronautical Laboratory, Inc.
4455 Genesee Street
Buffalo 21, New York
Attn: J. P. Desmond, Librarian

1 Sperry Gyroscope Company (Unclassified)
Marine Division Library
155 Glen Cove Road
Carle Place, L. I., New York
Attn: Mrs. Barbara Judd

1 Major William Harris
RADC (RAWI)
Griffiss Air Force Base
New York

1 Rome Air Development Center
Griffiss Air Force Base
New York
Attn: Documents Library
RAALD

1 Library (Unclassified)
Light Military Electronics Department
General Electric Company
Armament & Control Products Section
Johnson City, New York

1 Columbia Radiation Laboratory
Columbia University (Unclassified)
538 West 120th Street
New York 57, New York

1 Mr. Alan Barnum
Rome Air Development Center
Griffiss Air Force Base
Rome, New York

1 Dr. E. Howard Holt (Unclassified)
Director
Plasma Research Laboratory
Rensselaer Polytechnic Institute
Troy, New York

3 Commanding Officer
U.S. Army Research Office (Durham)
Box CM, Duke Station
Durham, North Carolina
Attn: CRD-AA-IP, Mr. Ulsh

1 Battelle-DEFENDER
Battelle Memorial Institute
505 King Avenue
Columbus 1, Ohio

1 Aeronautical Systems Division
Navigation and Guidance Laboratory
Wright-Patterson Air Force Base
Ohio

1 Aeronautical Systems Division
Directorate of Systems Dynamic Analysis
Wright-Patterson Air Force Base
Ohio

1 Commander
Research & Technology Div.
Wright-Patterson Air Force Base
Ohio 45433
Attn: MAYT (Mr. Evans)

1 Commanding Officer (AD-5)
U.S. Naval Air Development Center
Johnsville, Pennsylvania
Attn: NADC Library

2 Commanding Officer
Frankford Arsenal
Philadelphia 37, Pennsylvania
Attn: SMUFA-1300

1 H. E. Cochran
Oak Ridge National Laboratory
P. O. Box X
Oak Ridge, Tennessee

1 U.S. Atomic Energy Commission
Office of Technical Information Extension
P. O. Box 62
Oak Ridge, Tennessee

1 President
U.S. Army Air Defense Board
Fort Bliss, Texas

1 U.S. Air Force Security Service
San Antonio, Texas
Attn: ODC-R

1 Director
Human Resources Research Office
The George Washington University
300 North Washington Street
Alexandria, Virginia

20 Defense Documentation Center
Cameron Station
Alexandria, Virginia
22314

1 Commander
U. S. Army Research Office
Highland Building
3045 Columbia Pike
Arlington 4, Virginia

1 U.S. Naval Weapons Laboratory
Computation and Analysis Laboratory
Dahlgren, Virginia
Attn: Mr. Ralph A. Niemann

2 Army Material Command
Research Division
R & D Directorate
Bldg. T-7
Gravelley Point, Virginia